

Sharpened CG iteration bound for Schwarz-preconditioned high-contrast heterogeneous scalar elliptic PDEs

Going beyond condition number

WI5005: Thesis Project (Interim Thesis)

Philip Soliman

Sharpened CG iteration bound for Schwarz- preconditioned high-contrast heterogeneous scalar elliptic PDEs

Going beyond condition number

by

Philip Soliman

To obtain the degree of Master of Science
at the Delft University of Technology,
to be defended publicly on T.B.A.

Student number:	4945255	
Project duration:	December 2024 – September 2025	
Thesis committee:	Prof. H. Schuttelaars, Dr. A. Heinlein, F. Cumar,	TU Delft, responsible supervisor TU Delft, daily supervisor TU Delft, daily co-supervisor
Faculty:	Faculty of Electrical Engineering, Mathematics and Computer Science	
Department:	Numerical Analysis	

This thesis is confidential and cannot be made public until December 31, 2025.

Published on Tuesday 29th April, 2025

An electronic version of this thesis is available at <http://repository.tudelft.nl/>.

Contents

Nomenclature	ii
1 Introduction	1
2 Mathematical background	3
2.1 Conjugate Gradient Method	4
2.1.1 Variants of the CG method	5
2.1.2 Krylov subspaces	5
2.1.3 CG algorithm	5
2.1.4 CG convergence rate	6
2.1.5 Influence of eigenvalue distribution on CG convergence	7
2.1.6 Preconditioned CG	12
2.2 Schwarz Methods	13
2.2.1 Schwarz methods as preconditioners	14
2.2.2 Convergence of the original Schwarz method	15
2.2.3 Need for a coarse space	16
2.2.4 Two-level additive Schwarz method	17
2.2.5 Convergence of two-level additive Schwarz	19
3 Related Work	21
3.1 The spectral gap arising in Darcy problems	22
3.2 Tailored coarse spaces for high-contrast problems	22
3.2.1 MsFEM	22
3.2.2 ACMS	22
3.2.3 GDSW	23
3.2.4 AMS	23
3.3 CG convergence in case of non-uniform spectra	23
4 Research questions	25
4.1 Main research question	26
4.2 Subsidiary research questions	26
4.3 Motivation	26
4.4 Challenges	26
5 Preliminary Results	27
5.1 Two cluster case	28
5.2 Generalization to multiple clusters	30
5.3 Numerical experiments	32
5.4 Implications for research	34
6 Conclusion	35

Nomenclature

Symbols

Table 1: Symbols related to the heterogeneous elliptic problem.

Symbol	Description
Ω	Bounded domain in \mathbb{R}^d with Lipschitz boundary.
$\partial\Omega$	Boundary of Ω .
\mathbb{R}^d	d -dimensional Euclidean space.
C	Scalar coefficient in the Darcy problem, assumed to lie in $L^\infty(\Omega)$.
u	Exact solution of the elliptic problem.
f	Source term belonging to $L^2(\Omega)$.
u_D	Dirichlet boundary data.
κ_{\min}	Lower bound of the scalar coefficient κ .
κ_{\max}	Upper bound of κ .
u_h	Finite element approximation of u .
V_h	Finite-dimensional subspace of $H_0^1(\Omega)$.
$\{\phi_i\}_{i=1}^n$	Basis functions spanning V_h .
A	Stiffness matrix derived from the Galerkin method.
b	Load vector in the resulting linear system.
v_h	Test function in V_h .

Table 2: Symbols related to the Conjugate Gradient (CG) method.

Symbol	Description
\mathbf{u}_0	Initial guess for the solution.
\mathbf{r}_0	Initial residual defined as $\mathbf{b} - A\mathbf{u}_0$.
\mathbf{r}_j	Residual vector at the j^{th} iteration.
\mathbf{p}_j	Search direction at iteration j .
α_j	Step size computed at iteration j .
β_j	Coefficient used to update the search direction in iteration j .
$K_m(A, \mathbf{r}_0)$	Krylov subspace spanned by $\{\mathbf{r}_0, A\mathbf{r}_0, A^2\mathbf{r}_0, \dots, A^{m-1}\mathbf{r}_0\}$.
T_m	Tridiagonal Hessenberg matrix arising from the Lanczos process.
δ_j	Diagonal entries of T_m .
η_j	Off-diagonal entries of T_m .
\mathbf{e}_m	Error at iteration m , defined as $\mathbf{u}^* - \mathbf{u}_m$.
P_{m-1}	Space of polynomials of degree at most $m - 1$.
λ_i	Eigenvalues of A .
ξ_i	Components of the initial error in the eigenvector basis of A .
$\sigma(A)$	Spectrum (set of eigenvalues) of A .
C_m	Chebyshev polynomial of degree m .
ρ_0	Initial residual in the eigenvector basis of A .

Table 3: Symbols related to Schwarz preconditioners.

Symbol	Description
Ω_i	Subdomains obtained from partitioning Ω .
R_i	Restriction operator for subdomain Ω_i .

Symbol	Description
D_i	Diagonal matrix representing the partition of unity (weights) for Ω_i .
N_{sub}	Number of subdomains.
M_{ASM}^{-1}	Additive Schwarz preconditioner defined by $M_{ASM} = \sum_{i=1}^{N_{sub}} R_i^T (R_i A R_i^T)^{-1} R_i$.
M_{RAS}^{-1}	Restrictive Additive Schwarz preconditioner defined by $M_{RAS} = \sum_{i=1}^{N_{sub}} R_i^T D_i (R_i A R_i^T)^{-1} R_i$.
R_0	Restriction operator associated with the coarse space.
P_j	Local projection operator associated with subdomain Ω_j .
P_0	Projection operator for the coarse space.
P_{ad}	Sum of the projection operators, $P_{ad} = \sum_{j=1}^{N_{sub}} P_j$, used in the two-level method.
$\kappa(P_{ad})$	Condition number of the preconditioned system, given by $\frac{\lambda_{\max}}{\lambda_{\min}}$ of P_{ad} .

Table 4: Symbols related to eigenspectra and CG convergence bounds (chapter 5: Preliminary Results).

Symbol	Description
$\sigma_1(A)$	Two-cluster eigenspectrum of A , defined as the union of two intervals $[a, b] \cup [c, d]$.
$\sigma_2(A)$	Eigenspectrum comprising a main cluster and a tail of eigenvalues, with the tail denoted by N_{tail} .
$[a, b]$	Interval containing the first cluster of eigenvalues.
$[c, d]$	Interval containing the second cluster of eigenvalues.
N_{tail}	Number of eigenvalues in the tail cluster (when the spectrum has one cluster plus a tail).
$\hat{r}_p^{(i)}(x)$	Residual polynomial function for the i^{th} cluster, defined piecewise (for $i = 1$, via a scaled expression; for $i = 2$, as a product over tail eigenvalues).
$\hat{r}_{\bar{m}-p}(x)$	Residual polynomial function based on Chebyshev polynomials, corresponding to the complementary polynomial degree $\bar{m} - p$.
$C_p^{(i)}$	Cluster-specific Chebyshev polynomial of degree p , adapted to the eigenvalue distribution of the i^{th} cluster.
η_1	Upper bound for $\max_{x \in [a, b]} \hat{r}_p^{(1)}(x) $, given by $2 \left(\frac{\sqrt{b} - \sqrt{a}}{\sqrt{b} + \sqrt{a}} \right)^p$.
η_2	Upper bound for $\max_{x \in [a, b]} \hat{r}_p^{(2)}(x) $, expressed as $\left(\frac{b}{a} - 1 \right)^p$ when $p = N_{tail}$.
\bar{m}	Total degree of the composite residual polynomial $r_{\bar{m}}$, formed as the product $\hat{r}_p^{(i)}(x) \hat{r}_{\bar{m}-p}(x)$.
ϵ	Relative error, defined as $\ e_m\ _A / \ e_0\ _A$ at the m^{th} iteration.
$z_1^{(i,j)}, z_2^{(j)}$	Chebyshev coordinates in the frame of reference of the i^{th} cluster
k	Positive integer parameter in the Chebyshev inequality, corresponding to the degree in the bound estimate.
p_i	Chebyshev degree associated with the i^{th} eigenvalue cluster, determining the contraction factor of that cluster's contribution to the residual.
κ_i	Condition number of the i^{th} eigenvalue cluster, defined as the ratio of the largest to smallest eigenvalue within the cluster.

Symbol	Description
f_i	Convergence factor (or spectral measure) for the i^{th} cluster.

Abbreviations

Table 5: List of abbreviations and their full meanings.

Abbreviation	Full Meaning
CG	Conjugate Gradient
PCG	Preconditioned Conjugate Gradient
SPD	Symmetric Positive Definite
FEM	Finite Element Method
ASM	Additive Schwarz Method
RAS	Restrictive Additive Schwarz
ORAS	Optimized Restrictive Additive Schwarz
MsFEM	Multiscale Finite Element Method
ACMS	Approximate Component Mode Synthesis
GDSW	Generalized Dryja-Smith-Widlund
AMS	Algebraic Multiscale Solver
DtN	Dirichlet-to-Neumann
DBC	Dirichlet Boundary Condition
NBC	Neumann Boundary Condition
DOF(s)	Degree(s) of Freedom
PDE	Partial Differential Equation

1

Introduction

Reliable numerical simulation often requires solving large systems of equations. In many applications, most of the computational effort is spent on this task. Iterative solvers like Conjugate Gradient (CG) are widely used, but their efficiency heavily depends on the number of iterations required to reach convergence.

Preconditioners help reduce the iteration count. Choosing a good preconditioner is key to speeding up simulations. A common way to assess their performance is by looking at the condition number of the preconditioned system matrix. A smaller condition number usually means faster convergence.

But this measure is too general. In high-contrast heterogeneous problems, like those arising from the scalar Laplace equation with varying coefficient, the condition number does not capture important spectral features. For example, clusters of eigenvalues or large gaps in the spectrum often control the actual behavior of CG. This means that two systems with the same condition number can behave very differently in practice.

To improve preconditioner selection, we need better tools to predict performance. This leads to the central question of this thesis:

How can we refine the CG iteration bound for Schwarz-preconditioned high-contrast heterogeneous elliptic problems beyond the classical condition number-based bound?

To answer this central question, the thesis explores several sub-questions:

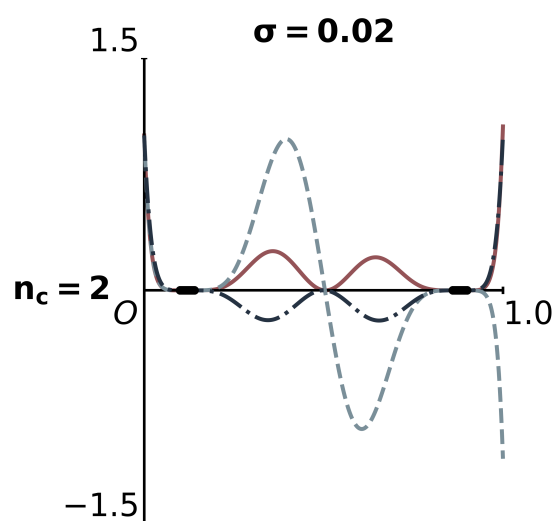
1. What spectral characteristics can be defined to better capture the eigenvalue distribution in these problems?
2. How can these characteristics be quantitatively estimated for a model heterogeneous coefficient Laplace problem?
3. What insights can be derived from the refined spectral characteristics to improve preconditioner selection?
4. How does the new bound compare with classical estimates, both with and without preconditioning?
5. Can the refined bounds help differentiate the performance of various Schwarz-like preconditioners?
6. How can these insights be used to derive a sharper CG iteration bound?

By addressing these questions, the thesis aims to improve the understanding of solver performance in challenging high-contrast settings. The results can guide better design and selection of preconditioners for faster, more reliable simulations.

This thesis is organized as follows. In chapter 2, the mathematical background of the CG method and Schwarz methods is introduced. chapter 3 reviews related work, providing context for the current study and highlighting differences between existing approaches. Chapter 4 details the research questions, motivation, and challenges associated with refining the CG iteration bound. Chapter 5 presents preliminary results that illustrate the potential benefits of the proposed approach. Finally, chapter 6 summarizes the key insights and discusses directions for future research.

2

Mathematical background



In this chapter we focus on a simple Darcy problem like the one posed in [1, 11]. This problem is of the form

$$\begin{aligned} -\nabla \cdot (\mathcal{C} \nabla u) &= f \quad \text{in } \Omega, \\ u &= u_D \quad \text{on } \partial\Omega, \end{aligned} \quad (2.1)$$

where $\Omega \subset \mathbb{R}^d$ is a bounded domain with Lipschitz boundary $\partial\Omega$, $\mathcal{C} \in L^\infty(\Omega)$ is a positive coefficient, $f \in L^2(\Omega)$ is a source term, and $u \in H_0^1(\Omega)$ is the solution. The coefficient \mathcal{C} is assumed to be bounded from above and below by positive constants, i.e., $0 < \mathcal{C}_{\min} \leq \mathcal{C}(x) \leq \mathcal{C}_{\max} < \infty$ for all $x \in \Omega$. The solution u is assumed to be sufficiently smooth, i.e., $u \in H^2(\Omega) \cap H_0^1(\Omega)$, so that the problem is well-posed. The goal is to compute an approximation $u_h \in V_h$ to the solution u using a finite-dimensional subspace $V_h \subset H_0^1(\Omega)$, where V_h is spanned by a set of basis functions $\{\phi_i\}_{i=1}^n$. The Galerkin method seeks $u_h \in V_h$ such that

$$\int_{\Omega} \mathcal{C} \nabla u_h \cdot \nabla v_h \, dx = \int_{\Omega} f v_h \, dx \quad \text{for all } v_h \in V_h. \quad (2.2)$$

The discretisation is done in the context of the finite element method. To that end we consider a triangulation \mathcal{T} of the domain Ω and a partition of unity χ_j . Denote by $V_{h,0} = V_h \cap H_0^1(\Omega)$ the space of piecewise continuous functions $v_h \in H_0^1(\Omega)$ with respect to \mathcal{T} . Let the basis of $V_{h,0}$ be given by $\{\phi_k\}_{k \in \mathcal{N}}$. The FE formulation of the Poisson problem equation (2.1) follows from the variational form

$$a(u_h, v_h) = (f, v_h), \quad \forall u_h, v_h \in V_{h,0},$$

and is given by

$$A\mathbf{u} = \mathbf{b}, \quad A_{ij} = a(\phi_j, \phi_i), \quad b_i = (f, \phi_i) \quad \forall i, j \in \mathcal{N}, \quad (2.3)$$

where A is the stiffness matrix, \mathbf{b} is the load vector and \mathcal{N} is the set of indices corresponding to the degrees of freedom. The stiffness matrix A is symmetric and positive definite, and the load vector \mathbf{b} is determined by the source term f and the boundary conditions.

Next to this we need a way of interpolating functions in $C(\Omega)$ to V_h . This is done by the interpolation operator $\mathcal{I}_h : C(\Omega) \mapsto V_{h,0}$, which is defined by

$$\mathcal{I}_h v = \sum_{i \in \mathcal{N}} v(x_i) \phi_i,$$

where x_i are the nodes of the triangulation \mathcal{T} . \mathcal{I}_h is stable with respect to the a -norm, that is

$$\|\mathcal{I}_h(v)\|_a \leq C_{\mathcal{I}_h} \|v\|_a.$$

The solution \mathbf{u} can be computed using iterative methods like the conjugate gradient method, which is guaranteed to converge in a finite number of iterations for symmetric positive definite matrices in infinite precision arithmetic.

2.1. Conjugate Gradient Method

The CG method is a special instance of the class of Krylov subspace methods. It is derived from the Direct Lanczos (D-Lanczos) algorithm applied to the residual of linear systems [17, Algorithm 6.17]. The D-Lanczos algorithm generates a sequence of orthonormal Lanczos vectors $\{\mathbf{v}_1, \mathbf{v}_2, \dots, \mathbf{v}_m\}$ that span the Krylov subspace $\mathcal{K}_m(A, \mathbf{r}_0)$, where $\mathbf{r}_0 = \mathbf{b} - A\mathbf{u}_0$ is the initial residual such that

$$\mathcal{K}_m(A_0, \mathbf{r}_0) = \text{span}\{\mathbf{r}_0, A\mathbf{r}_0, A^2\mathbf{r}_0, \dots, A^{m-1}\mathbf{r}_0\}, \quad (2.4)$$

or \mathcal{K}_m as a shorthand. The approximate answer is then given by

$$\mathbf{u}_m = \mathbf{u}_0 + \sum_{i=0}^{m-1} c_i A^i \mathbf{r}_0 = \mathbf{u}_0 + q_{m-1}(A) \mathbf{r}_0, \quad (2.5)$$

where $q_{m-1}(A)$ is a polynomial of degree $m-1$ in A . It is shown later in this section how the coefficients c_i are obtained (equation (2.16)).

2.1.1. Variants of the CG method

Variants of the CG method differ in the way A is preconditioned (see section 2.1.6) and the choices for the constraint subspace \mathcal{L}_m . The former type of variations result in the preconditioned CG method (PCG) and these are described in section 2.1.6. The latter type of variations further separate into two major categories:

- i $\mathcal{L}_m = \mathcal{K}_m$ and $\mathcal{L}_m = A\mathcal{K}_m$;
- ii $\mathcal{L}_m = \mathcal{K}_m(A^T, \mathbf{r}_0)$.

Note that item CG-type i correspond to the residual and error projection methods. The former results in Arnoldi's method, as well as variants thereof like Full Orthogonalization Method (FOM), Incomplete Orthogonalization Method (IOM) and Direct Incomplete Orthogonalization Method (DIOM). The latter on the other hand results in the Generalized Minimum Residual Method (GMRES).

2.1.2. Krylov subspaces

Definition 2.1. The grade of a vector v with respect to a matrix A is the lowest degree of the polynomial q such that $q(A)v = 0$.

Consequently,

Theorem 2.1. The Krylov subspace \mathcal{K}_m is of dimension m if and only if the grade μ of v with respect to A is not less than m [17, proposition 6.2],

$$\dim(\mathcal{K}_m) = m \iff \mu \geq m,$$

such that

$$\dim(\mathcal{K}_m) = \min\{m, \text{grade}(v)\}. \quad (2.6)$$

2.1.3. CG algorithm

We can write the conjugate gradient method as algorithm 1.

Algorithm 1 Conjugate Gradient Method [17, Algorithm 6.18]

```

 $\mathbf{r}_0 = b - A\mathbf{u}_0, p_0 = \mathbf{r}_0, \beta_0 = 0$ 
for  $j = 0, 1, 2, \dots, m$  do
   $\alpha_j = (\mathbf{r}_j, \mathbf{r}_j) / (A p_j, p_j)$ 
   $\mathbf{u}_{j+1} = \mathbf{u}_j + \alpha_j p_j$ 
   $\mathbf{r}_{j+1} = \mathbf{r}_j - \alpha_j A p_j$ 
   $\beta_j = (\mathbf{r}_{j+1}, \mathbf{r}_{j+1}) / (\mathbf{r}_j, \mathbf{r}_j)$ 
   $p_{j+1} = \mathbf{r}_{j+1} + \beta_j p_j$ 
end for

```

The Lanczos vectors are related through the Lanczos recurrence relation

$$\eta_{j+1}(A)\mathbf{v}_{j+1} = A\mathbf{v}_j - \delta_j\mathbf{v}_j - \eta_j\mathbf{v}_{j-1}, \quad (2.7)$$

such that

$$T_m = \mathbf{v}_m^T A \mathbf{v}_m,$$

where T_m is the tridiagonal Hessenberg matrix given by

$$T_m = \begin{pmatrix} \delta_1 & \eta_2 & 0 & \dots & 0 \\ \eta_2 & \delta_3 & \eta_3 & \dots & 0 \\ 0 & \eta_3 & \delta_4 & \dots & 0 \\ \vdots & \vdots & \vdots & \ddots & \eta_m \\ 0 & 0 & 0 & \eta_m & \delta_m \end{pmatrix}. \quad (2.8)$$

The following relations exist between the entries of T_m and the CG coefficients α_j, β_j

$$\delta_{j+1} = \begin{cases} \frac{1}{\alpha_j} + \frac{\beta_{j-1}}{\alpha_{j-1}} & j > 0, \\ \frac{1}{\alpha_0} & j = 0, \end{cases} \quad (2.9)$$

and

$$\eta_{j+1} = \frac{\sqrt{\beta_{j-1}}}{\alpha_{j-1}}. \quad (2.10)$$

Here we have used the definition of T_m and the fact that the residuals are multiples of the Lanczos vectors $\mathbf{r}_j = \text{scalar} \times \mathbf{v}_j$ [17, Equation 6.103].

2.1.4. CG convergence rate

We have the following theorem for the convergence rate of the CG algorithm

Theorem 2.2. The error of the m^{th} iterate of the CG algorithm is bounded by

$$\|\mathbf{e}_m\| \leq 2 \left(\frac{\sqrt{\kappa} - 1}{\sqrt{\kappa} + 1} \right)^m \|\mathbf{e}_0\|_A, \quad (2.11)$$

where $\kappa = \lambda_{\max}/\lambda_{\min}$ is the condition number of (symmetric matrix) A .

Proof. It can be shown [17, lemma 6.28 and theorem 6.29] that the error of the m^{th} iterate of the CG algorithm $\mathbf{e}_m = x^* - \mathbf{u}_m$ minimizes the A -norm of the error in the affine Krylov subspace $\mathcal{K}_m(A, \mathbf{r}_0)$, that is

$$\|(I - Aq_{m-1}(A))\mathbf{e}_0\|_A = \min_{q \in \mathcal{P}_{m-1}} \|(I - Aq(A))\mathbf{e}_0\|_A = \min_{r \in \mathcal{P}_m, r(0)=1} \|r(A)\mathbf{e}_0\|_A, \quad (2.12)$$

where the equality follows, since there exists an isomorphic mapping between the affine Krylov subspace and the polynomial space \mathcal{P}_{m-1} of degree $m-1$ and the polynomial $tq(t)$ equals 0 at $t=0$. The right-hand side can be further bounded by letting λ_i, ξ_i be the eigenvalues of A and the components of \mathbf{e}_0 in the eigenvector basis of A , respectively. Then

$$\|r(A)\mathbf{e}_0\|_A = \sqrt{\sum_{i=1}^n |r(\lambda_i)|^2 |\xi_i|^2} \leq \max_{\lambda \in \sigma(A)} |r(\lambda)| \|\mathbf{e}_0\|_A,$$

where $\sigma(A)$ is the spectrum of A . Given the eigenvalues are uniformly distributed in the interval $[\lambda_{\min}, \lambda_{\max}]$, we can bound the error of the m^{th} iterate of the CG algorithm as follows

$$\begin{aligned} \|\mathbf{e}_m\|_A &\leq \min_{r \in \mathcal{P}_{m-1}, r(0)=1} \max_{\lambda \in [\lambda_{\min}, \lambda_{\max}]} |r(\lambda)| \|\mathbf{e}_0\|_A \\ \text{Chebyshev polynomial } C_m, \eta &= \frac{\lambda_{\min}}{\lambda_{\max} - \lambda_{\min}} \rightarrow \frac{\|\mathbf{e}_0\|_A}{C_m(1+2\eta)} \\ &\leq \frac{2\|\mathbf{e}_0\|_A}{\left(1 + 2\eta + 2\sqrt{\eta(\eta+1)}\right)^m} \\ &= \frac{2\|\mathbf{e}_0\|_A}{\left(\sqrt{\eta} + \sqrt{\eta+1}\right)^{2m}} \\ &= 2 \left(\frac{\sqrt{\kappa} - 1}{\sqrt{\kappa} + 1} \right)^m \|\mathbf{e}_0\|_A, \end{aligned}$$

□

where $\kappa = \lambda_{\max}/\lambda_{\min}$ is the condition number of (the symmetric matrix) A . During the derivation of theorem 2.2, we obtain the general expression for the error of the m^{th} iterate of the CG algorithm

$$\|\mathbf{e}_m\| \leq \min_{r \in \mathcal{P}_m, r(0)=1} \max_{\lambda \in \sigma(A)} |r(\lambda)| \|\mathbf{e}_0\|_A$$

Now define,

$$r_{\text{test}}(t) = \prod_{i=1}^m \frac{\lambda_i - t}{\lambda_i}.$$

Note that $r_{\text{test}} \in \mathcal{P}_m$, since it has degree m . Also, $r_{\text{test}}(0) = 1$ and $r_{\text{test}}(\lambda_i) = 0$ for $i = 1, 2, \dots, m$. Hence, r_{test} is a polynomial that satisfies the constraints of the minimization problem. We obtain for $m = N$ that

$$\|\mathbf{e}_N\|_A = \|\mathbf{e}_0\|_A \max_{\lambda \in \sigma(A)} |r_{\text{test}}(\lambda)| = 0,$$

which implies that CG converges in N iterations in exact arithmetic. Furthermore, if there are only k distinct eigenvalues, then the CG iteration terminates in at most k iterations.

2.1.5. Influence of eigenvalue distribution on CG convergence

In the derivation of the convergence rate of the CG algorithm, we used the Chebyshev polynomial to bound the error. However, we can find an expression of the error provided the eigendecomposition of A is available. Supposing A is full rank and by its symmetry we can write its diagonalization as $A = VDV^T$, where V is the orthonormal eigenvector matrix and D is the diagonal eigenvalue matrix. Then $r(A) = I - Aq(A) = V(I - Dq(D))V^T = Vr(D)V^T$. Also note that $\mathbf{e}_0 = x^* - \mathbf{u}_0 = A^{-1}b - \mathbf{u}_0 = A^{-1}\mathbf{r}_0$. As seen in equation (2.12), the error of the m^{th} iterate of the CG algorithm is given by

$$\|\mathbf{e}_m\|_A^2 = \|r_m(A)\mathbf{e}_0\|_A^2,$$

and

$$\begin{aligned} \|r_m(A)\mathbf{e}_0\|_A^2 &= \mathbf{e}_0^T r_m(A)^T A r_m(A) \mathbf{e}_0 \\ &= \mathbf{e}_0^T V r_m(D) V^T V D V^T V r_m(D) V^T \mathbf{e}_0 \\ &= (V^T \mathbf{e}_0)^T r_m(D) D r_m(D) V^T \mathbf{e}_0. \end{aligned}$$

We also have

$$\begin{aligned} V^T \mathbf{e}_0 &= V^T A^{-1} \mathbf{r}_0 \\ &= V^T V D^{-1} V^T \mathbf{r}_0 \\ &= D^{-1} \rho_0, \end{aligned}$$

where $\rho_0 = V^T \mathbf{r}_0$ is the initial residual in the eigenvector basis of A . Therefore,

$$\begin{aligned} \|r_m(A)\mathbf{e}_0\|_A^2 &= \rho_0^T D^{-1} r_m(D) D r_m(D) D^{-1} \rho_0 \\ &= \rho_0^T r_m(D) D^{-1} r_m(D) \rho_0 \\ &= \sum_{i=1}^n \frac{r_m(\lambda_i)^2}{\lambda_i} \rho_{0,i}^2, \end{aligned}$$

which gives

$$\|\mathbf{e}_m\|_A^2 = \sum_{i=1}^n \frac{r_m(\lambda_i)^2}{\lambda_i} \rho_{0,i}^2. \quad (2.13)$$

To obtain the residual polynomial r_m , we can use the recurrence relation between the Lanczos vectors and expressions for the Hessenberg matrix coefficients in equations (2.9) and (2.10). In particular,

$$\begin{aligned} \frac{1}{\eta_{j+1}} \mathbf{v}_{j+1} &= A \mathbf{v}_j - \delta_j \mathbf{v}_j - \eta_j \mathbf{v}_{j-1} \\ &= p_{j+1}(A) \mathbf{v}_1, \end{aligned}$$

where we define $p_{-1}(A) = 0, p_0(A) = I$. This gives

$$\begin{aligned} \eta_{j+1} p_{j+1}(A) \mathbf{v}_1 &= A \mathbf{v}_j - \delta_j \mathbf{v}_j - \eta_j \mathbf{v}_{j-1}, \\ &= (A p_j(A) - \delta_j p_j(A) - \eta_j p_{j-1}(A)) \mathbf{v}_1, \end{aligned}$$

and therefore

$$p_{j+1}(A) = \frac{1}{\eta_{j+1}} ((A - \delta_j)p_j(A) - \eta_j p_j(A)). \quad (2.14)$$

Furthermore, we have the following relation between the residual polynomial and the Lanczos polynomial [16, Section 3.2]

$$r_j(A) = (I - Aq_{j-1}(A))\mathbf{r}_0 = \frac{p_j(A)}{p_j(0)}\mathbf{r}_0. \quad (2.15)$$

This gives a way of calculating the residual polynomial r_m and thereby the error of the m^{th} iterate of the CG algorithm.

Additionally, the coefficients c_i of the solution polynomial q_m in equation (2.5) can be calculated. First we introduce a function that extracts the coefficients of a polynomial p

Definition 2.2. Let $p(t) = \sum_{i=0}^n c_i t^i$ be a polynomial of degree n . Then, the function $\text{coeff}(p; i)$ extracts the i^{th} coefficient of p such that $\text{coeff}(p; i) = c_i$.

Now using equation (2.15), we can write the solution polynomial as

$$\begin{aligned} Aq_{m-1}(A) &= I - r_m(A) \\ r_m(\mathbf{0}) = I &\implies A \sum_{i=1}^{m-1} c_{i-1} A^i = - \sum_{i=1}^m \text{coeff}(r_m; i) A^i, \end{aligned}$$

which implies

$$c_i = -\text{coeff}(r_m; i+1), \quad i = 0, 1, \dots, m-1. \quad (2.16)$$

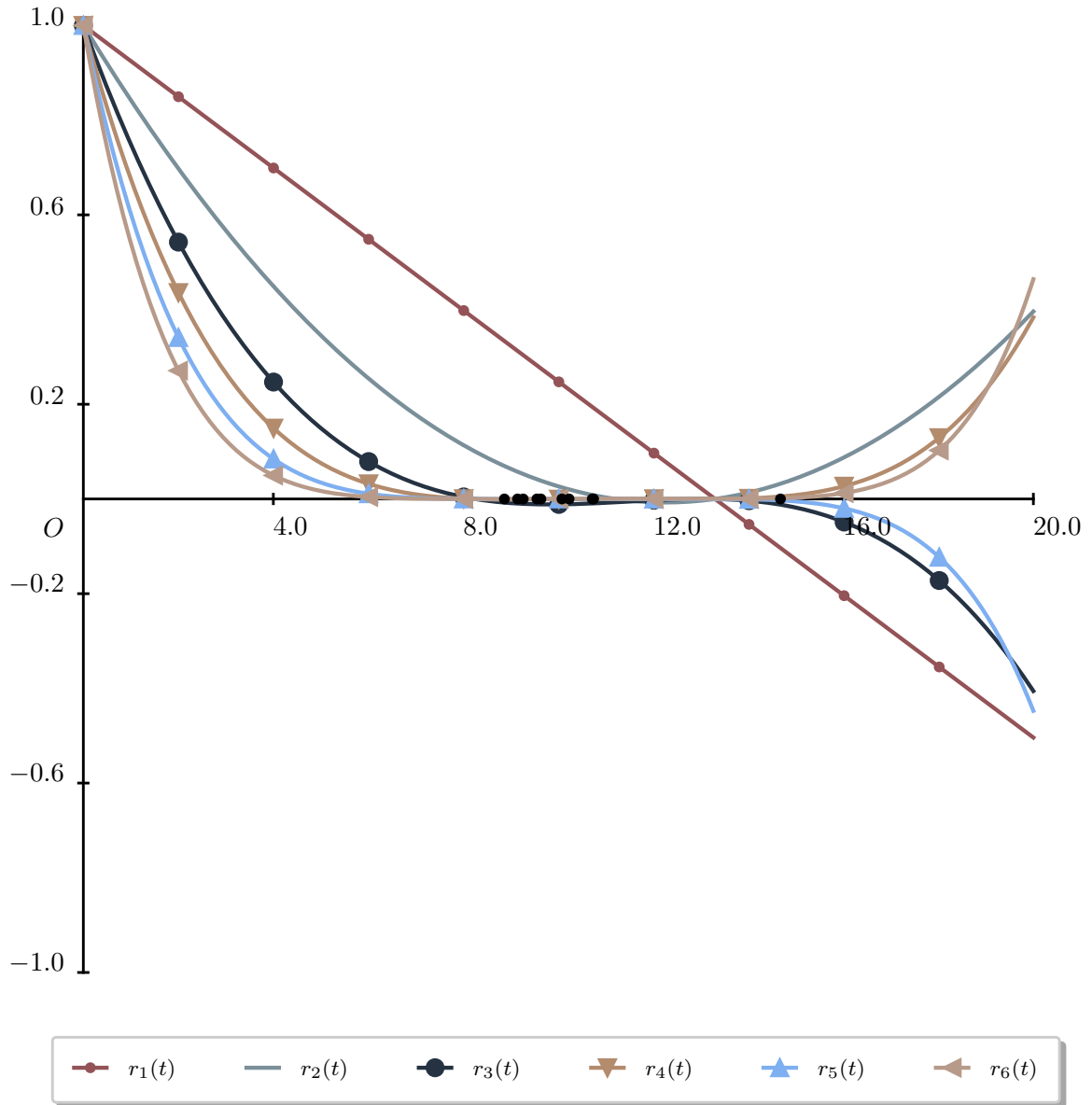


Figure 2.1: Residual polynomials resulting from successive CG iterations

The behavior of the residual polynomials is crucial for understanding the convergence properties of the CG method. In particular, the distribution of the eigenvalues of A significantly affects the convergence rate, as illustrated in figure 2.2. For all plots the lowest and highest eigenvalue in figure 2.2 are $\lambda_{\min} = 0.1$,

$\lambda_{\max} = 0.9$ such that $f = \frac{\sqrt{\frac{\lambda_{\min}}{\lambda_{\max}}} - 1}{\sqrt{\frac{\lambda_{\min}}{\lambda_{\max}}} + 1}$ and the ratio $\frac{\|\mathbf{e}_m\|_A}{\|\mathbf{e}_0\|_A}$ is set to $\frac{10^{-6}}{\|\mathbf{u}_{\text{test}} - \mathbf{u}_0\|}$. The system size $N = 360$

is kept small and the system matrix A is diagonal so that it is numerically trivial to determine the exact solution \mathbf{u}_{test} . This results in an overall iteration bound

$$m_{\text{classical}} = \left\lceil \log_f \left(\frac{10^{-6}}{2\|\mathbf{u}_{\text{test}} - \mathbf{u}_0\|} \right) \right\rceil = 26$$

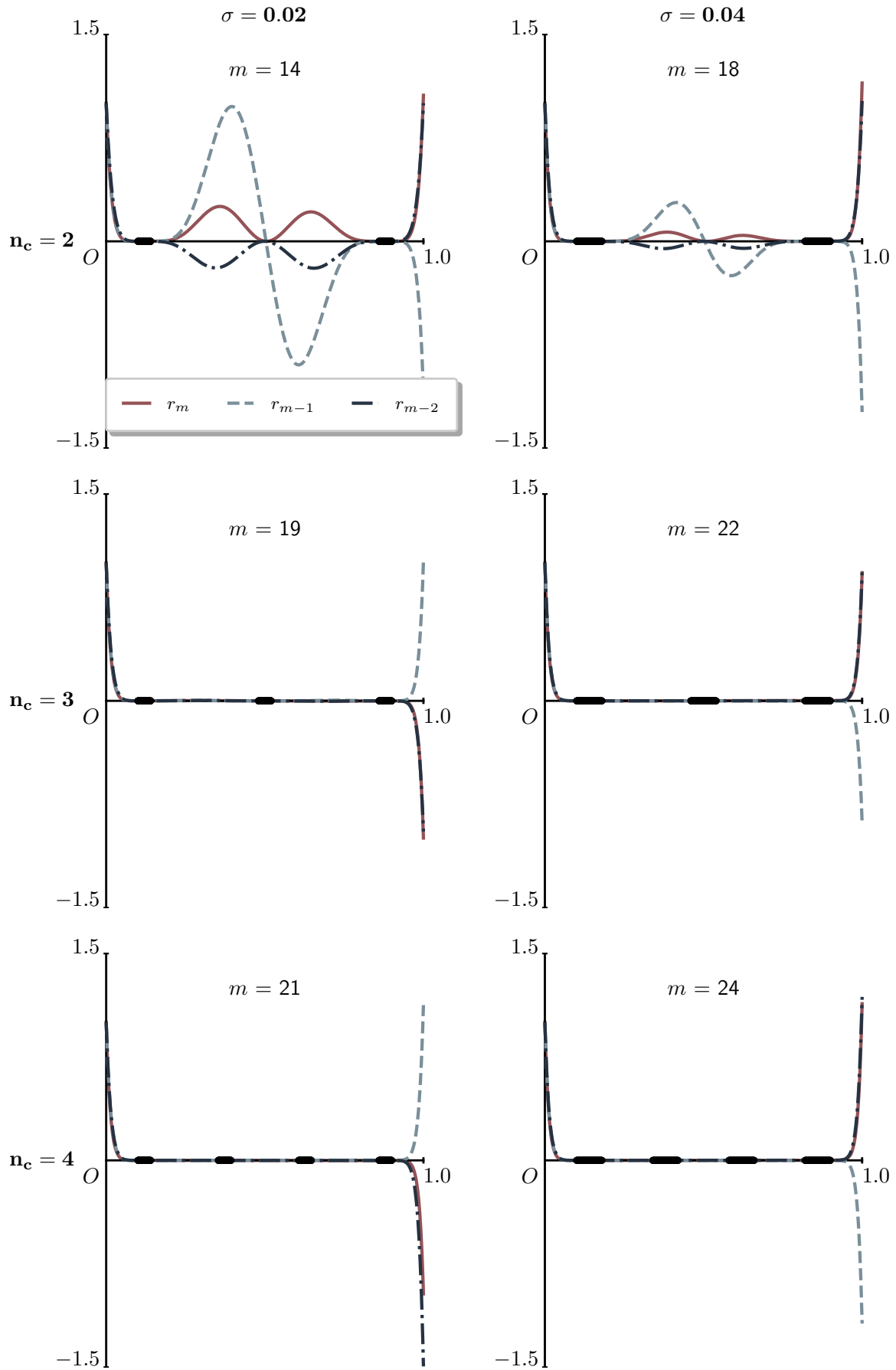


Figure 2.2: Plots of the last three CG residual polynomials for different eigenvalue distributions. n_c indicates the number of clusters and σ is the width of the cluster. The size of the system N and the condition number $\kappa(A)$ are kept constant. m indicates the number of iterations required for convergence.

Hence, the number of iterations required for convergence depends on the specific clustering of the eigenvalues, as pointed out for example in Kelley, Section 2.3.

Based behavior exhibited in figure 2.2 and from theorem 2.1, we can reason what the best and worst possible spectra for CG convergence are. That is, the best possible spectrum is one where eigenvalues are tightly clustered around distinct values, while the worst possible spectrum is one where the eigenvalues are evenly distributed across the whole range of the spectrum. This is illustrated in figure 2.3.

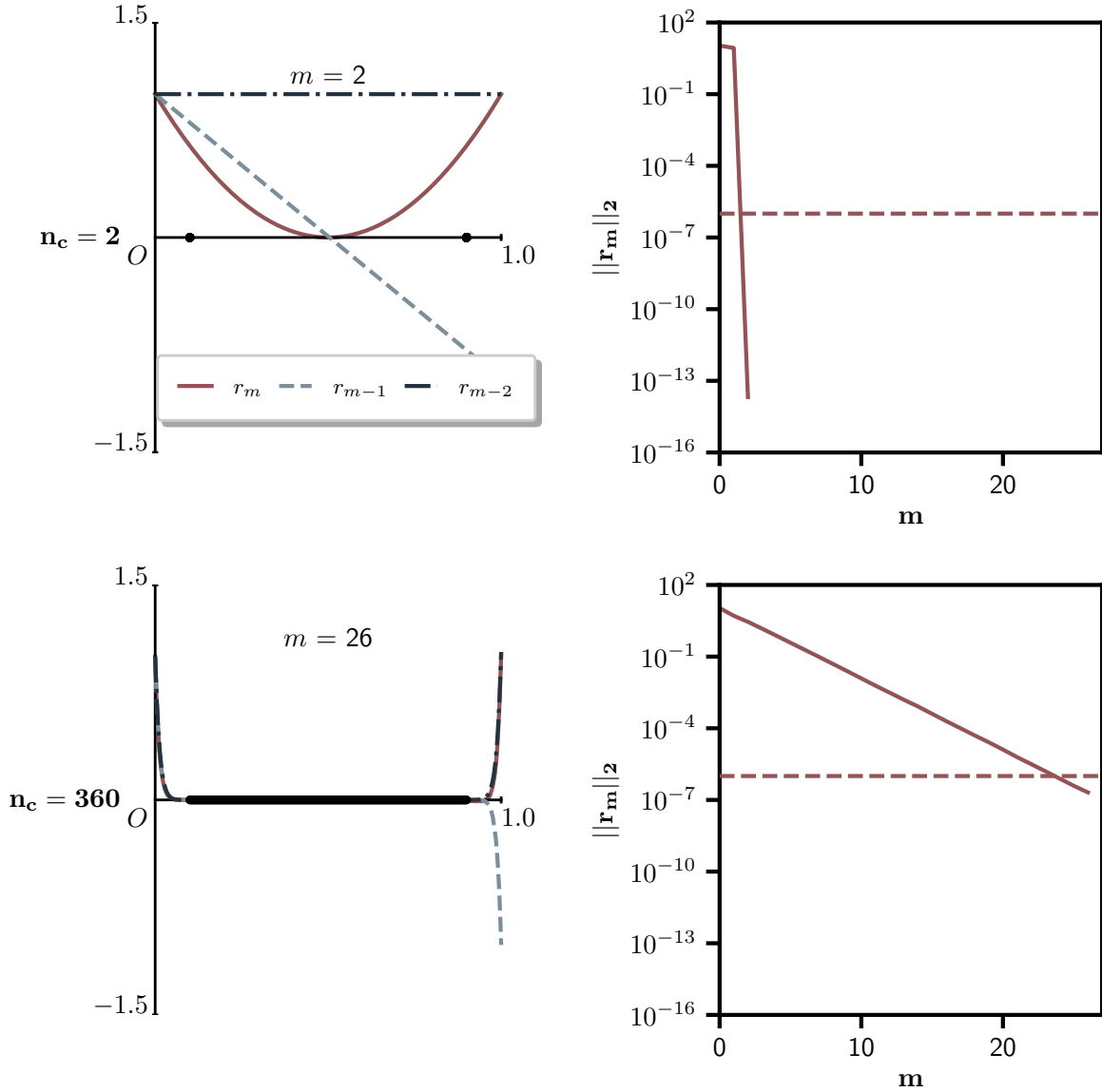


Figure 2.3: Best and worst possible spectra for CG convergence. The top row shows the best possible spectrum, where the eigenvalues are tightly clustered on two distinct values. The bottom row shows the worst possible spectrum, where the eigenvalues are evenly distributed across the whole range of the spectrum. The left column shows the eigenvalue distribution with the residual polynomials corresponding to the iteration. The right column shows the norm of the residual versus the iteration number. Convergence is achieved at a tolerance of 10^{-6} .

The first row in figure 2.3 shows an instance of the super-linear convergence that CG can exhibit, particularly when the eigenvalues are closely clustered. This is characteristic of CG is further touched upon in chapters 3 and 5.

2.1.6. Preconditioned CG

Suppose M is some SPD preconditioner, then variants of CG can be derived by applying M to the system of equations. The three main approaches are

PCG-1 left

$$M^{-1}A\mathbf{u} = M^{-1}\mathbf{b}$$

PCG-2 right

$$\begin{aligned} AM^{-1}\mathbf{x} &= M^{-1}\mathbf{b} \\ \mathbf{u} &= M^{-1}\mathbf{x}; \end{aligned}$$

PCG-3 symmetric or split

$$\begin{aligned} M &= LL^T \\ L^{-1}AL^{-T}\mathbf{x} &= L^{-1}\mathbf{b} \\ \mathbf{u} &= L^{-T}\mathbf{x}. \end{aligned}$$

Furthermore, all these variants are mathematically equivalent. Indeed, for the cases **PCG-type 1** and **PCG-type 2**, we can rewrite the CG algorithm using the M - or M^{-1} -inner products, respectively. In either case the iterates are the same. For instance for the left preconditioned CG, we define $\mathbf{z}_j = M^{-1}\mathbf{r}_j$. Note that $M^{-1}A$ is self-adjoint with respect to the M -inner product, that is for $\mathbf{x}, \mathbf{y} \in \mathbb{R}^n$ we have

$$(M^{-1}A\mathbf{x}, \mathbf{y})_M = (A\mathbf{x}, \mathbf{y}) = (\mathbf{x}, A\mathbf{y}) = (\mathbf{x}, M^{-1}A\mathbf{y})_M.$$

We use this to get a new expression for α_j . To that end, we write

$$\begin{aligned} 0 &= (\mathbf{r}_{j+1}, \mathbf{r}_j)_M \\ &= (\mathbf{z}_{j+1}, \mathbf{r}_j) \\ &= (\mathbf{z}_j - \alpha_j M^{-1}A\mathbf{p}_j, M^{-1}\mathbf{r}_j)_M \\ &= (\mathbf{z}_j, M^{-1}\mathbf{r}_j)_M - \alpha_j (M^{-1}A\mathbf{p}_j, M^{-1}\mathbf{r}_j)_M \\ &= (\mathbf{z}_j, \mathbf{z}_j)_M - \alpha_j (M^{-1}A\mathbf{p}_j, \mathbf{z}_j)_M \end{aligned}$$

and therefore

$$\alpha_j = \frac{(\mathbf{z}_j, \mathbf{z}_j)_M}{(M^{-1}A\mathbf{p}_j, \mathbf{z}_j)_M}.$$

Using $\mathbf{p}_{j+1} = \mathbf{z}_{j+1} + \beta_j \mathbf{p}_j$ and A-orthogonality of the search directions \mathbf{p}_j with respect to M -norm $(A\mathbf{p}_j, \mathbf{p}_k)_M = 0$, we can write

$$\alpha_j = \frac{(\mathbf{z}_j, \mathbf{z}_j)_M}{(M^{-1}A\mathbf{p}_j, \mathbf{p}_j)_M}.$$

Similarly, we can derive the equivalent expression for β_j as

$$\beta_j = \frac{(\mathbf{z}_{j+1}, \mathbf{z}_{j+1})_M}{(\mathbf{z}_j, \mathbf{z}_j)_M}.$$

This gives the left preconditioned CG algorithm in 2.

Algorithm 2 Left preconditioned CG [17, Algorithm 9.1]

```

 $\mathbf{r}_0 = \mathbf{b} - A\mathbf{u}_0, \mathbf{z}_0 = M^{-1}\mathbf{r}_0, p_0 = \mathbf{z}_0, \beta_0 = 0$ 
for  $j = 0, 1, 2, \dots, m$  do
   $\alpha_j = (\mathbf{z}_j, \mathbf{z}_j)_M / (M^{-1}A\mathbf{p}_j, \mathbf{p}_j)_M = (\mathbf{r}_j, \mathbf{z}_j) / (A\mathbf{p}_j, \mathbf{p}_j)$ 
   $\mathbf{u}_{j+1} = \mathbf{u}_j + \alpha_j \mathbf{p}_j$ 
   $\mathbf{r}_{j+1} = \mathbf{r}_j - \alpha_j A\mathbf{p}_j$ 
   $\mathbf{z}_{j+1} = M^{-1}\mathbf{r}_{j+1}$ 
   $\beta_j = \frac{(\mathbf{z}_{j+1}, \mathbf{z}_{j+1})_M}{(\mathbf{z}_j, \mathbf{z}_j)_M} = \frac{(\mathbf{r}_{j+1}, \mathbf{z}_{j+1})}{(\mathbf{r}_j, \mathbf{z}_j)}$ 
   $\mathbf{p}_{j+1} = \mathbf{z}_{j+1} + \beta_j \mathbf{p}_j$ 
end for

```

Furthermore it can be shown that the iterates of CG applied to the system with **PCG-type 3** results in identical iterates [17, Algorithm 9.2].

2.2. Schwarz Methods

The content of this section is largely based on chapters 1, 2, 4 and 5 of Dolean, Jolivet, and Nataf about Schwarz methods.

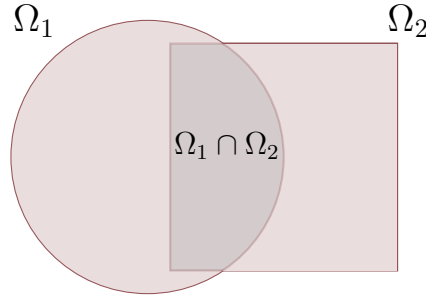


Figure 2.4: Keyhole domain Ω with two overlapping subdomains Ω_1 and Ω_2 . The boundary of the keyhole domain is denoted by $\partial\Omega$ and the boundaries of the subdomains are denoted by $\partial\Omega_1$ and $\partial\Omega_2$. The overlapping region is denoted by $\Omega_1 \cap \Omega_2$.

The original Schwarz method was a way of proving that a Poisson problem on some complex domain Ω as in figure 2.4 has a solution.

$$\begin{aligned} -\Delta u &= f \text{ in } \Omega, \\ u &= 0 \text{ on } \partial\Omega. \end{aligned} \tag{2.17}$$

Existence of a solution is proved by splitting up the original complex domain in two (or more) simpler, possibly overlapping subdomains and solving the Poisson problem on each of these subdomains. The solution on the original domain is then the sum of the solutions on the subdomains. The method is named after Hermann Schwarz, who first introduced the method in 1869 [18]. The method has since been extended to more general problems and is now a popular method for solving partial differential equations. Let the alternating Schwarz method be characterised as in definition 2.3.

Definition 2.3. The Alternating Schwarz algorithm is an iterative method based on alternately solving subproblems in domains Ω_1 and Ω_2 . It updates $(u_1^n, u_2^n) \rightarrow (u_1^{n+1}, u_2^{n+1})$ by

$$\begin{aligned} -\Delta (u_1^{n+1}) &= f & \text{in } \Omega_1, & & -\Delta (u_2^{n+1}) &= f & \text{in } \Omega_2, \\ u_1^{n+1} &= 0 & \text{on } \partial\Omega_1 \cap \partial\Omega, & \text{then} & u_2^{n+1} &= 0 & \text{on } \partial\Omega_2 \cap \partial\Omega, \\ u_1^{n+1} &= u_2^n & \text{on } \partial\Omega_1 \cap \overline{\Omega_2}, & & u_2^{n+1} &= u_1^{n+1} & \text{on } \partial\Omega_2 \cap \overline{\Omega_1}. \end{aligned}$$

The original Schwarz algorithm is sequential and, thereby, does not allow for parallelization. However, the algorithm can be parallelized. The Jacobi Schwarz method is a generalization of the original Schwarz method, where the subproblems are solved simultaneously and subsequently combined into a global

solution. In order to combine local solutions into one global solution, an extension operator E_i , $i = 1, 2$ is used. It is defined as

$$E_i(v) = v \text{ in } \Omega_i, \quad E_i(v) = 0 \text{ in } \Omega \setminus \Omega_i.$$

Instead of solving for local solutions directly, one can also solve for local corrections stemming from a global residual. This is the additive Schwarz method (ASM). It is defined in algorithm 3.

Algorithm 3 Additive Schwarz method [8, Algorithm 1.2]

Compute residual $r^n = f - \Delta u^n$.

For $i = 1, 2$ solve for a local correction v_i^n :

$$-\Delta v_i^n = r^n \text{ in } \Omega_i, \quad v_i^n = 0 \text{ on } \partial\Omega_i$$

Update the solution: $u^{n+1} = u^n + \sum_{i=1}^2 E_i(v_i)^n$.

The restricted additive Schwarz method (RAS) is similar to ASM, but differs in the way local corrections are combined to form a global one. In the overlapping region of the domains it employs a weighted average of the local corrections. In particular, a partition of unity χ_i is used. It is defined as

$$\chi_i(x) = \begin{cases} 1, & x \in \Omega_i \setminus \Omega_{3-i}, \\ 0, & x \in \delta\Omega_i \setminus \delta\Omega \\ \alpha, & 0 \leq \alpha \leq 1, x \in \Omega_i \cap \Omega_{3-i} \end{cases}$$

such that for any function $w : \Omega \rightarrow \mathbb{R}$, it holds that

$$w = \sum_{i=1}^2 E_i(\chi_i w_{\Omega_i}).$$

The RAS algorithm is defined in algorithm 4.

Algorithm 4 Restrictive additive Schwarz method [8, Algorithm 1.1]

Compute residual $r^n = f - \Delta u^n$.

For $i = 1, 2$ solve for a local correction v_i^n :

$$-\Delta v_i^n = r^n \text{ in } \Omega_i, \quad v_i^n = 0 \text{ on } \partial\Omega_i$$

Update the solution: $u^{n+1} = u^n + \sum_{i=1}^2 E_i(\chi_i v_i^n)$.

2.2.1. Schwarz methods as preconditioners

Let \mathcal{N} be set containing all indices of degrees of freedom in the domain Ω and N_{sub} be the number of subdomains such that

$$\mathcal{N} = \sum_{i=1}^{N_{\text{sub}}} \mathcal{N}_i,$$

\mathcal{N}_i is the set of indices of degrees of freedom in the subdomain Ω_i .

Furthermore, let $R_i \in \mathcal{R}^{|\mathcal{N}_i| \times |\mathcal{N}|}$, R_i^T and D_i be the discrete versions of the restriction, extension and partition of unity operators such that

$$\mathcal{R}^{|\mathcal{N}|} \ni U = \sum_{i=1}^{N_{\text{sub}}} R_i^T D_i R_i U.$$

Note that D_i is a diagonal matrix where the entries are the values of the partition of unity function χ_i evaluated for each degree of freedom. Consider for instance, a multidimensional FEM problem, in

which \mathcal{T} is the triangulation of the domain Ω and \mathcal{T}_i is the triangulation of the subdomain Ω_i such that [8, Equation 1.27]

$$\Omega_i = \cup_{\tau \in \mathcal{T}_i} \tau.$$

In this case [8, Equation 1.28]

$$\mathcal{N}_i = \{k \in \mathcal{N} | \text{meas}(\text{supp}(\phi_k) \cap \Omega_i) > 0\},$$

and we can define

$$\mu_k = |\{j | 1 \leq j \leq N_{\text{sub}} \text{ and } k \in \mathcal{N}_j\}|.$$

Finally, this leads to

$$(D_i)_{kk} = \frac{1}{\mu_k}, \quad k \in \mathcal{N}_i. \quad (2.18)$$

Although the original Schwarz method is not a preconditioner, the ASM and RAS methods can be used as such. Originally the Schwarz method is a fixed point iteration [8, Definitions 1.12 and 1.13]

$$u^{n+1} = u^n + M^{-1}r^n, \quad r^n = f - Au^n,$$

where M equals, but is not limited to, one of the following matrices;

$$M_{\text{ASM}}^{-1} = \sum_{i=1}^{N_{\text{sub}}} R_i^T (R_i A R_i^T)^{-1} R_i, \quad (2.19a)$$

$$M_{\text{RAS}}^{-1} = \sum_{i=1}^{N_{\text{sub}}} R_i^T D_i (R_i A R_i^T)^{-1} R_i. \quad (2.19b)$$

Both M_{ASM}^{-1} and M_{RAS}^{-1} are SPD and can be used as preconditioners for CG.

Optimized Schwarz methods and corresponding preconditioners can also be constructed by including more interface conditions (Robin or Neumann) in the subproblems. One such example is the Optimized Restrictive Additive Schwarz method (ORAS) discussed in [8, Chapter 2].

2.2.2. Convergence of the original Schwarz method

In this section the Schwarz problem stated in definition 2.3 is solved in the one- and two-dimensional case. The convergence of the original Schwarz method is then discussed.

1D case

Let $L > 0$ and the domain $\Omega = (0, L)$. The domain is split into two subdomains $\Omega_1 = (0, L_1)$ and $\Omega_2 = (l_2, L)$ such that $l_2 \leq L_1$. Instead of solving for $u_{1,2}$ directly, we solve for the error $e_{1,2}^n = u_{1,2}^n - u|_{\Omega_i}$, which by linearity of the Poisson problem as well as the original Schwarz algorithm satisfies

$$\begin{aligned} -\frac{e_1^{n+1}}{dx^2} &= f \text{ in } (0, L_1), & -\frac{e_2^{n+1}}{dx^2} &= f \text{ in } (l_2, L), \\ e_1^{n+1}(0) &= 0, & \text{then } e_2^{n+1}(l_2) &= e_1^{n+1}(l_2), \\ e_1^{n+1}(L_1) &= e_2^n(L_1); & e_2^{n+1}(L) &= 0. \end{aligned}$$

The solution to the error problem is

$$e_1^{n+1}(x) = \frac{x}{L_1} e_2^n(L_1), \quad e_2^{n+1}(x) = \frac{L-x}{L-l_2} e_1^{n+1}(l_2).$$

These functions increase linearly from the boundary of the domain to the boundary of the overlapping region. The error at $x = L_1$ is updated as

$$e_2^{n+1}(L_1) = \frac{1 - \delta/(L-l_2)}{1 + \delta/l_2} e_2^n(L_1),$$

where $\delta = L_1 - l_2 > 0$ is the overlap. The error is reduced by a factor of

$$\rho_{1D} = \frac{1 - \delta/(L-l_2)}{1 + \delta/l_2}, \quad (2.20)$$

which indicates the convergence becomes quicker as the overlap increases [8, Section 1.5.1].

2D case

In the 2D case two half planes are considered $\Omega_1 = (-\infty, \delta) \times \mathbb{R}$ and $\Omega_2 = (\delta, \infty) \times \mathbb{R}$. Following the example of Dolean, Jolivet, and Nataf the problem is

$$\begin{aligned} -(\eta - \Delta)u &= f \text{ in } \mathbb{R}^2, \\ u &\text{ bounded at infinity,} \end{aligned}$$

where $\eta > 0$ is a constant. Proceeding in similar fashion as the one-dimensional case, the error $e_{1,2}^{n+1}$ can be solved for in the two subdomains. This is done via a partial Fourier transform of the problem in the y-direction yielding an ODE for the transformed error $\hat{e}_{1,2}^{n+1}$ with the added Fourier constant k , which can be solved explicitly with the ansatz

$$\hat{e}_{1,2}^{n+1}(x, k) = \gamma_1(k)e^{\lambda_+(k)x} + \gamma_2(k)e^{\lambda_-(k)x},$$

where $\lambda_{\pm}(k) = \pm\sqrt{k^2 + \eta}$. By using the interface conditions we find

$$\gamma_i^{n+1}(k) = \rho(k; \eta, \delta)^2 \gamma_i^{n-1}(k),$$

such that the convergence factor is [8, Equation 1.36]

$$\rho_{2D}(k; \eta, \delta) = e^{-\delta\sqrt{\eta+k^2}} \quad (2.21)$$

which indicates that the convergence is quicker as the overlap increases as before. Next to this, it also shows that the convergence is quicker for higher k .

2.2.3. Need for a coarse space

Following upon the results in the previous section 2.2.2 it is clear that the convergence of the Schwarz method not only depends on the extent of the overlap between various subdomains, but on the frequency components of the solution as well. In a general sense this means that low frequency modes need for instance at least N_{sub} steps to travel from one end of a square domain to the other. This in turns causes plateaus in the convergence of the Schwarz method. To overcome this, we can perform a Galerkin projection of the error onto a coarse space. By solving

$$\min_{\beta} \|A(\mathbf{u} + R_0^T \beta) - f\|^2,$$

where R_0 is a matrix representing the coarse space. The solution to this problem is

$$\beta = (R_0 A R_0^T)^{-1} R_0 r,$$

where $r = f - A\mathbf{u}$ is the residual.

The coarse space R_0 can be constructed in various ways. The classical way is called the Nicolaides space [8, Section 4.2], which uses the discrete partition of unity operators D_i as exemplified in equation (2.18) to get

$$R_0 = \sum_{i=1}^{N_{\text{sub}}} R_i^T D_i R_i. \quad (2.22)$$

Note that the coarse space has a block-diagonal form.

Finally the coarse space correction term can be added to the Schwarz preconditioners equations (2.19a) and (2.19b) to get the following preconditioners

$$M_{\text{ASM},2} = R_0^T (R_0 A R_0^T)^{-1} R_0 + \sum_{i=1}^{N_{\text{sub}}} R_i^T (R_i A R_i^T)^{-1} R_i, \quad (2.23a)$$

$$M_{\text{RAS},2} = R_0^T (R_0 A R_0^T)^{-1} R_0 + \sum_{i=1}^{N_{\text{sub}}} R_i^T D_i (R_i A R_i^T)^{-1} R_i. \quad (2.23b)$$

2.2.4. Two-level additive Schwarz method

In this section we will construct a coarse space for a Poisson problem with a constant scalar coefficient on arbitrary domain like in problem 2.17. However, the method is applicable to more general (highly) heterogeneous scalar problems, like the Darcy problem. The coarse space is constructed using the eigenfunctions corresponding to the smallest m_j eigenvalues resulting from a local eigenproblem in each subdomain Ω_j . The coarse space is then constructed by taking the union of the m_j eigenvectors corresponding to the smallest eigenvalues in each subdomain glued together by the partition of unity functions χ_j . All of this can be found in [8, Sections 5.1-5.5].

This coarse space is subsequently used to construct the two level additive Schwarz preconditioner, and bounds for its condition number are provided as well.

Slowly convergent modes of the Dirichlet-to-Neumann map

As seen in section 2.2.2 the local error in any subdomain in the Schwarz method satisfies the homogeneous version of the original problem, i.e. right hand side $f = 0$. At the interface the local error has a Dirichlet boundary condition that equals the error of the neighbouring subdomain. Additionally, the convergence factor, e.g. ρ_{2D} , depends on the frequency of the modes in the local error. In particular, small frequencies appear to have slow convergence. The question thus becomes how to get rid of these small frequency modes in the local errors of all subdomains.

One possible answer is the so-called Dirichlet-to-Neumann map [8, Definition 5.1]

Definition 2.4. (Dirichlet-to-Neumann map for a Poisson problem) For any function defined on the interface $u_{\Gamma_j} : \Gamma_j \mapsto \mathbb{R}$, we consider the Dirichlet-to-Neumann map

$$\text{DtN}_{\Omega_j}(u_{\Gamma_j}) = \frac{\partial v}{\partial \mathbf{n}_j} \Big|_{\Gamma_j},$$

where $\Gamma_j := \partial\Omega_j \setminus \partial\Omega$ and v satisfies

$$\begin{aligned} -\Delta v &= 0 && \text{in } \Omega_j, \\ v &= u_{\Gamma_j} && \text{on } \Gamma_j, \\ v &= 0 && \text{on } \partial\Omega_j \cap \partial\Omega. \end{aligned} \tag{2.24}$$

The Dirichlet-to-Neumann map essentially solves for an error-like variable v that satisfies the Dirichlet local interface (or global boundary) conditions. DtN then maps the interface condition to the normal derivative of v on the interface, i.e. the Neumann condition. Now, as stated above and illustrated in [8, Figure 5.2] the low frequency modes of the error correspond to those modes that are nearly constant across an interface, for which the Neumann condition is close to zero. So the problem of slowly convergent modes in the error of the Schwarz method is equivalent to a problem of finding eigenpairs of the DtN operator.

Hence we aim to solve the eigenvalue problem

$$\text{DtN}_{\Omega_j}(v) = \lambda v,$$

which can be reformulated in the variational form. To that end let w be a test function that is zero on $\delta\Omega$. Multiply both sides of equation (2.24) by w , integrate over Ω_j and apply Green's theorem to get

$$\int_{\Omega_j} \nabla v \cdot \nabla w - \lambda \int_{\Gamma_j} \frac{\partial v}{\partial \mathbf{n}_j} w = 0, \quad \forall w.$$

Then, use the eigen property of v and fact that w is zero on Γ_j to get the eigen problem in the variational form

$$\text{Find } (v, \lambda) \text{ s.t. } \int_{\Omega_j} \nabla v \cdot \nabla w - \lambda \int_{\Gamma_j} v w = 0, \quad \forall w. \tag{2.25}$$

Construction of Two-level additive Schwarz preconditioner

As before we partition Ω into N_{sub} subdomains Ω_j , which overlap each other by one or several layers of elements in the triangulation \mathcal{T} . We make the following observations

D1 For every degree of freedom $k \in \mathcal{N}$, there is a subdomain Ω_j such that ϕ_k has support in Ω_j [8, Lemma 5.3].

D2 The maximum number of subdomains a mesh element can belong to is given by

$$k_0 = \max_{\tau \in \mathcal{T}} (|\{j | 1 \leq j \leq N_{\text{sub}} \text{ and } \tau \subset \Omega_j\}|).$$

D3 The minimum number of colors needed to color all subdomains so that no two adjacent subdomains have the same color is given by

$$N_c \geq k_0$$

D4 The minimum overlap for any subdomain Ω_j with any of its neighboring subdomains is given by

$$\delta_j = \inf_{x \in \Omega_j \setminus \bigcup_{i \neq j} \bar{\Omega}_i} \text{dist}(x, \partial\Omega_j \setminus \partial\Omega).$$

D5 The partition of unity functions $\{\chi_j\}_{j=1}^{N_{\text{sub}}} \subset V_h$ are such that

D5.a $\chi_j(x) \in [0, 1], \quad \forall x \in \bar{\Omega}, j = 1, \dots, N_{\text{sub}},$

D5.b $\text{supp}(\chi_j) \subset \bar{\Omega}_j,$

D5.c $\sum_{j=1}^{N_{\text{sub}}} \chi_j(x) = 1, \quad \forall x \in \bar{\Omega},$

D5.d $\|\nabla \chi_j(x)\| \leq \frac{C_\chi}{\delta_j},$

and are given by

$$\chi_j(x) = I_h \left(\frac{d_j(x)}{\sum_{j=1}^{N_{\text{sub}}} d_j(x)} \right),$$

where

$$d_j(x) = \begin{cases} \text{dist}(x, \partial\Omega_j), & x \in \Omega_j, \\ 0, & x \in \Omega \setminus \Omega_j. \end{cases}$$

D6 The overlap region for any subdomain is given by

$$\Omega_j^\delta = \{x \in \Omega_j | \chi_j < 1\}.$$

From item **D1** it follows that the extension operator $E_j : V_{h,0}(\Omega_j) \rightarrow V_h$ can be defined by

$$V_h = \sum_{j=1}^{N_{\text{sub}}} E_j V_{h,0}(\Omega_j).$$

Note that using the extension operator we can show that all the local bilinear forms are positive definite as

$$a_{\Omega_j}(v, w) = a(E_j v, E_j w) \geq \alpha \|E_j v\|_a^2, \quad \forall v, w \in V_{h,0}(\Omega_j),$$

and a is positive definite.

Finally, we define the a -symmetric projection operators $\tilde{\mathcal{P}}_j : V_{h,0} \rightarrow V_h$ and $\mathcal{P}_j : V_h \rightarrow V_h$ defined by

$$\begin{aligned} a_{\Omega_j}(\tilde{\mathcal{P}}_j u, v_j) &= a(u, E_j v_j) \quad \forall v_j \in V_{h,0}, \\ \mathcal{P} &= E_j \tilde{\mathcal{P}}_j. \end{aligned}$$

Then their matrix counterparts are given by

$$\begin{aligned} \tilde{P}_j &= A_j^{-1} R_j^T A, \\ P_j &= R_j^T A_j^{-1} R_j^T A, \end{aligned}$$

where $A_j = R_j A R_j^T$. From this we can construct the two-level additive Schwarz method as

$$M_{\text{ASM},2}^{-1} A = \sum_{j=1}^{N_{\text{sub}}} P_j. \quad (2.26)$$

2.2.5. Convergence of two-level additive Schwarz

In the following we denote

$$\mathcal{P}_{\text{ad}} = \sum_{j=1}^{N_{\text{sub}}} \mathcal{P}_j,$$

and correspondingly,

$$P_{\text{ad}} = \sum_{j=1}^{N_{\text{sub}}} P_j.$$

In the context of this thesis the two-level additive Schwarz method is used in combination with a Krylov subspace method, in which case convergence rate depends on the entire spectrum of eigenvalues (section 2.1.5). However, an upperbound for the convergence rate (section 2.1.4) can be derived from the condition number of P_{ad} via equation (2.12).

Using the fact that P_{ad} is symmetric (see [8, Lemma 5.8]) with respect to the a -norm, we can write

$$\kappa(P_{\text{ad}}) = \frac{\lambda_{\max}}{\lambda_{\min}},$$

where

$$\lambda_{\max} = \sup_{v \in V_h} \frac{a(\mathcal{P}_{\text{ad}})}{a(v, v)}, \quad \lambda_{\min} = \inf_{v \in V_h} \frac{a(\mathcal{P}_{\text{ad}})}{a(v, v)}.$$

Additionally, we can employ the a -orthogonality of the projection operators to get

$$\frac{a(\mathcal{P}_j u, u)}{\|u\|_a^2} = \frac{a(\mathcal{P}_j u, \mathcal{P}_j u)}{\|u\|_a^2} \leq 1.$$

Going further, we can pose that the projection operators defined by the sum of projection operators \mathcal{P}_j of like-colored subdomains are a -orthogonal to each other. This is due to the fact that the partition of unity functions χ_j are such that they are zero on the interface of like-colored subdomains (see item **D3**). To that end, define

$$\mathcal{P}_{\Theta_i} = \sum_{j \in \Theta_i} \mathcal{P}_j,$$

where Θ_i is the set of indices of subdomains with color i and $i = 1, \dots, N_c$. Then, we can write [8, Lemma 5.9]

$$\begin{aligned} \lambda_{\max}(\mathcal{P}_{\text{ad}}) &= \sup_{v \in V_h} \sum_{i=1}^{N_c} \frac{a(\mathcal{P}_{\Theta_i} v, v)}{a(v, v)} \\ &\leq \sum_{i=1}^{N_c} \sup_{v \in V_h} \frac{a(\mathcal{P}_{\Theta_i} v, v)}{a(v, v)} \\ &\leq N_c + 1, \end{aligned}$$

where the extra one comes from the coarse projection operator \mathcal{P}_0 . Note that this bound can be made sharper by using item **D2** to get $\lambda_{\max}(\mathcal{P}_{\Theta_i}) \leq k_0 + 1$.

On the other hand, it can be shown that the minimum eigenvalue satisfies provided that $v \in V_h$ admits a C_0 -stable decomposition [8, Theorem 5.11]

$$\lambda_{\min}(\mathcal{P}_{\text{ad}}) \geq C_0^{-2}.$$

Finally, we can write the condition number of the two-level additive Schwarz preconditioner as

$$\kappa(P_{\text{ad}}) \leq (N_c + 1) C_0^2. \quad (2.27)$$

The value of C_0 depends on the projection operator Π_j onto the chosen coarse space V_0 for each subdomain.

I. **Nicolaides coarse space** The projection operator is defined as

$$\Pi_j^{\text{Nico}} u = \begin{cases} \left(\frac{1}{|\Omega_j|} \int_{\Omega_j} u \right) \mathbf{1}_{\Omega_j}, & \delta\Omega_j \cap \delta\Omega = \emptyset, \\ 0, & \text{otherwise,} \end{cases} \quad (2.28)$$

which gives rise to the following basis functions in $V_{h,0}$

$$\Phi_j^{\text{Nico}} = I_h(\chi_j \mathbf{1}_{\Omega_j}).$$

Then,

$$V_0 = \text{span}\{\Phi_j^{\text{Nico}}\}_{j=1}^{N_{\text{sub}}},$$

and

$$\dim V_0 = \text{the number of floating subdomains,}$$

that is the number of subdomains that are not connected to the boundary of the domain Ω . In this case [8, Theorem 5.16]

$$C_0^2 = \left(8 + 8C_\chi^2 \max_{j=1}^{N_{\text{sub}}} \left[C_P^2 + C_{\text{tr}}^{-1} \frac{H_j}{\delta_j} \right] k_0 C_{I_h}(k_0 + 1) + 1 \right), \quad (2.29)$$

where H_j is the diameter of the subdomain Ω_j , C_P the Poincaré constant following from [8, Lemma 5.18] and C_{tr} is the trace constant.

II. **Local eigenfunctions coarse space** The projection operator is defined as

$$\Pi_j^{\text{spec}} u = \sum_{k=1}^{m_j} a_{\Omega_j}(u, v_k^{(j)}) v_k^{(j)},$$

where $v_k^{(j)}$ is the k^{th} eigenfunction resulting from the eigenproblem in equation (2.25). The basis functions in $V_{h,0}$ are then given by

$$\Phi_{j,k}^{\text{spec}} = I_h(\chi_j v_k^{(j)}),$$

resulting in the coarse space

$$V_0 = \text{span}\{\Phi_{j,k}^{\text{spec}}\}_{j=1, k=1}^{N_{\text{sub}}, m_j},$$

with dimension

$$\dim V_0 = \sum_{j=1}^{N_{\text{sub}}} m_j.$$

In this case [8, Theorem 5.17]

$$C_0^2 = \left(8 + 8C_\chi^2 \max_{j=1}^{N_{\text{sub}}} \left[C_P^2 + C_{\text{tr}}^{-1} \frac{1}{\delta_j \lambda_{m_j+1}} \right] k_0 C_{I_h}(k_0 + 1) + 1 \right). \quad (2.30)$$

3

Related Work

3.1. The spectral gap arising in Darcy problems

In a Darcy problem, high-contrast $\mathcal{C}(x)$ (e.g., 10^6 in conductive channels vs. 10^{-6} in barriers) means flow concentrates in high-permeability regions, while low-permeability zones resist flow. This heterogeneity introduces modes (eigenvectors) that are nearly constant or slowly varying over low- $\mathcal{C}(x)$ regions, contributing small eigenvalues to A . These modes represent “trapped” or “isolated” behaviors disconnected by the contrast.

Small eigenvalues arise when the bilinear form $a(u, v) = \int_{\Omega} \mathcal{C}(x) \nabla u \cdot \nabla v \, dx$ yields low energy for certain test functions v . In high-contrast cases, if $\mathcal{C}(x)$ is extremely low in a subdomain, ∇u must be large there to balance the equation, but FEM basis functions often cannot resolve this without fine meshes. Instead, coarse bases produce modes where energy is minimized, leading to eigenvalues close to zero. This is exacerbated as contrast grows, adding more such modes.

High-contrast $\mathcal{C}(x)$ can split the spectrum into clusters: large eigenvalues tied to high- $\mathcal{C}(x)$ regions (where gradients dominate) and small eigenvalues tied to low- $\mathcal{C}(x)$ regions (where flow stagnates). In [9], the authors note that standard FEM misses these small eigenvalues unless enriched bases capture fine-scale features.

3.2. Tailored coarse spaces for high-contrast problems

Various methods for constructing a coarse space that are both scalable and robust to high contrast in a problem coefficient.

3.2.1. MsFEM

The Multiscale Finite Element Method (MsFEM), as presented in [9, 10, 13], constructs a coarse space based on five key assumptions (C1-C5). These assumptions ensure stability and accuracy by defining how the coarse space interacts with the fine-scale problem. Local coarse grid basis functions are obtained by solving the homogeneous version of the system equation, meaning they do not include external forcing terms. The construction of these basis functions requires specific boundary conditions, categorized as M1-M4, which control their behavior at interfaces. The method distinguishes between linear and oscillatory boundary conditions for local problems, affecting the resulting coarse space. Coarse grid basis functions are computed as harmonic extensions of basis functions restricted to edges or faces, ensuring continuity across subdomains. The restriction operator R_0 is then derived from these basis functions, as given in Equation 2.12 of [10]. Additionally, the method introduces robustness indicators, $\pi(\alpha)$ and $\gamma(\alpha)$, to quantify the stability of the coarse space and its effectiveness in capturing fine-scale features.

3.2.2. ACMS

The Approximate Component Mode Synthesis (ACMS) method, detailed in [11], introduces a separation of scales with fine and coarse triangulations, denoted as \mathcal{T}_h and \mathcal{T}_H . The coarse problem is decomposed into two components: $u_c = u_I + u_{\Gamma}$, where u_I and u_{Γ} represent the interior and interface contribution, respectively. This extends MsFEM by incorporating vertex-specific, edge-specific, and fixed-interface basis functions, where MsFEM corresponds solely to the vertex-specific functions. The vertex-specific basis functions are defined as harmonic extensions of trace values on the interface set Γ . Edge-specific basis functions, on the other hand, arise from an eigenvalue problem defined on an edge e , while fixed-interface basis functions correspond to eigenmodes of an eigenvalue problem within a coarse element T .

ACMS supports two types of coarse spaces, depending on whether Dirichlet (DBC) or Neumann (NBC) boundary conditions are applied. Under DBCs, MsFEM basis functions are combined with edge-specific basis functions that match on a shared edge e_{ij} between subdomains Ω_i and Ω_j . These functions are constructed from the harmonic extension of eigenmodes defined on the edge e_{ij} , with a scaled bilinear form on the right-hand side. Only eigenmodes corresponding to eigenfrequencies below a set tolerance are retained. With NBCs, both MsFEM and edge-specific basis functions are modified. MsFEM functions remain defined on an edge e_{ij} and satisfy a Kronecker-delta vertex condition but are now obtained via a generalized eigenvalue problem on a slab of width kh , denoted η_{ij}^{kh} . The edge-specific functions are similarly defined through a generalized eigenvalue problem on the slab but without enforcing DBCs. Solving these eigenvalue problems can be computationally efficient by

employing mass matrix lumping techniques.

3.2.3. GDSW

The Generalized Dryja-Smith-Widlund (GDSW) method, introduced by [6], partitions the computational domain into non-overlapping subdomains and further divides degrees of freedom (DOFs) into interior and interface nodes. The only required input for the method is a coarse space G . G corresponds to the null space of the problem. In the case of linear elasticity, G spans the rigid body modes, while for the diffusion problem the null space is a constant function. The restriction operators R_Γ and R_I project onto interface and interior DOFs, respectively, with subdomain-specific versions such as R_{Γ_j} .

The coarse problem matrix is [1, Equation 2]

$$A_0 = \Phi^T A \Phi,$$

where, by ordering the DOFs of into interface Γ and interior I nodes we can get [1, Equation 4, 5]

$$\Phi = \begin{pmatrix} -A_{II}^{-1} A_{I\Gamma} \\ I_{\Gamma\Gamma} \end{pmatrix} \Phi_\Gamma,$$

in which Φ_Γ is the prolongation operator of the interface nodes. The coarse solution on the interface set is subsequently defined as

$$u_{0,\Gamma} = \sum_j^{N_{\text{sub}}} R_{\Gamma_j}^T G_{\Gamma_j} q_j = \Phi_\Gamma q,$$

where q represents the coarse space coefficients. The complete coarse solution is then given by

$$u_0 = \Phi_\Gamma^T u_{0,\Gamma} + \Phi_I^T u_{0,I},$$

where $\Phi_I = -A_{II}^{-1} A_{I\Gamma} \Phi_\Gamma$ is computed by discrete harmonic extension.

RGDSW

The RGDSW method alters the GDSW preconditioner by reducing the coarse space dimension through a partitioning strategy based on nodal equivalence classes that associates each coarse mesh vertex with interface components formed by adjacent edges and faces, distributed among nearby vertices [7]. This reduction in the dimension of the coarse space is achieved without compromising the robustness of the condition number estimate, ensuring that the preconditioner's convergence properties are maintained [12].

3.2.4. AMS

The Algebraic Multiscale Solver (AMS) method, introduced in [15, 20] and further studied in [1], also relies on domain decomposition into non-overlapping subdomains, followed by a further subdivision of interface nodes into edge, vertex, and face nodes (in 3D). The method eliminates lower diagonal blocks in the system matrix to facilitate efficient computation. Like (R)GDSW, AMS employs the energy minimization principle to obtain Φ_I , ensuring an optimal coarse space representation.

3.3. CG convergence in case of non-uniform spectra

Excessive work has been done on the convergence rate of the CG method, especially in the context of non-uniform spectra. The following papers provide valuable insights into this topic.

First, in [2] a clever use of Chebyshev polynomials is demonstrated to obtain a sharpened CG iteration bound for two kinds of eigenspectra. This technique is further developed in section 5.1, providing additional insights into the convergence behavior of CG.

Second, in [19] the convergence rate of CG is investigated in the case of non-uniform spectra. The authors show that the convergence rate strongly depends on the eigenvalue distribution of the matrix A . By examining a parametrized class of matrices, they study how small perturbations in eigenvalues impact CG performance. Their experiments reveal that there exists a critical value of a parameter at which the number of iterations required for convergence greatly exceeds the degrees of freedom N , even when the condition number is small ($K = 100$) and N is small (e.g., 12 or 24). Moreover, this critical

value shifts with increasing precision, so that higher precision reduces the impact of rounding errors. The study further shows that the CG behavior is consistent across different algorithm variants (standard CG, SYMMQL, Jacobi acceleration, etc.). These results suggest that certain eigenvalue distributions make CG highly sensitive to numerical errors, and they underline the importance of preconditioners that can modify the eigenvalue distribution to improve CG robustness in practical applications.

Third, in [5] the authors provide a proof of CG's superlinear convergence. They explain why the conjugate gradient method exhibits faster (superlinear) convergence than the classical bound suggests. In particular, they derive a new asymptotic error bound that is sharper than the standard estimate. This new bound is expressed via the integral [5, Equation 1.8]:

$$\frac{1}{m} \log \left(\min_{r \in \mathcal{P}_m, r(0)=1} \max_{\lambda \in \sigma(A)} |r(\lambda)| \right) \lesssim -\frac{1}{t} \int_0^t g_{S(\tau)}(0) d\tau, \quad (3.1)$$

where $t = \frac{m}{N}$, $S(\tau)$ is a family of sets determined by the eigenvalue distribution and g_S is the Green function for the complement of S with pole at ∞ . As shown by equation (3.1) and theorem 2.1 in [3], the error is bounded by a term that decreases more quickly as the number of iterations increases. Under additional separation conditions among eigenvalues (see Theorem 2.2), the bound is proven to be asymptotically sharp. Moreover, for matrices with equidistant eigenvalues, an explicit formula [5, Corollary 3.2 and Equation 3.11] confirms the improved rate and aligns with observed CG error curves. These findings help to explain why, in practice, CG converges faster than predicted by traditional condition number bounds.

Fourth, in [3] the authors present a proof of the sharpness of the CG iteration bound equation (3.1). The paper shows that one cannot beat the asymptotic error estimate bound obtained earlier. It analyzes a strategy in which zeros of the polynomial are set at all eigenvalues outside a chosen set S . The authors prove that any such polynomial cannot yield a better asymptotic error bound than the one given by the earlier formula. They use a constrained energy problem from logarithmic potential theory to define the optimal set $S(t)$. Under conditions that are natural for problems arising from discretized PDEs on the eigenvalue distribution, the bound is demonstrated to be sharp, and the discussion includes cases where equality in the bound is reached.

Finally, in [4] the authors extend the results of [5] to cases where the eigenvalue distribution is asymptotically uniform. They show that even when the asymptotic distribution equals an equilibrium distribution, the CG method can exhibit superlinear convergence. In this work, the superlinearity stems from the particular choice of the right-hand side b . The authors present a family of examples based on the finite difference discretization of the one-dimensional Poisson problem, where they observe superlinear convergence according to the chosen right-hand sides.

4

Research questions

4.1. Main research question

The main research question in this work is as follows:

Research Question. How can we sharpen the CG iteration bound for Schwarz-preconditioned high-contrast heterogeneous scalar-elliptic problems beyond the classical condition number-based bound?

For instance, in [1], the AMS and GDSW preconditioners significantly outperform the RGDSW preconditioner, despite all three having similar condition numbers. The key differences appear in their spectral gap and cluster width, highlighting the need for additional spectral characteristics to refine existing bounds.

4.2. Subsidiary research questions

Subsidiary Questions. To answer the main research question, we address the following subsidiary questions:

- Q1** What spectral characteristics, like the condition number, can we define to estimate the distribution of eigenvalues in the eigenspectrum in the case of high-contrast heterogeneous problems?
- Q2** How can we estimate any of the spectral characteristics defined in **Q1** for the eigenspectrum in the particular case of a model Darcy problem?
- Q3** Given a certain eigenspectrum, how can we sharpen the CG iteration bound?
- Q4** How does the sharpened bound from **Q3** perform for an unpreconditioned Darcy problem in comparison with the classical bound in equation (2.12)?
- Q5** How does the performance described in **Q4** of a sharpened bound vary with the measures found in **Q1**?
- Q6** How can we employ the sharpened bound to distinguish between the performance of Schwarz-like preconditioners?

4.3. Motivation

This research is important because current studies primarily focus on selecting between different Schwarz preconditioners for the Darcy problem, yet condition numbers fail to distinguish them effectively. The ability to differentiate preconditioners based on spectral properties would improve the selection process. Applying sharpened bounds could lead to better predictions of preconditioner performance and improved efficiency in solving high-contrast problems.

4.4. Challenges

The main challenge lies in quantitatively estimating the spectrum of the preconditioned system. The literature provides a priori condition number estimates for various Schwarz preconditioners. For instance, in the simple cases of the additive Schwarz preconditioner with either a **ASM type I coarse space** or **ASM type II coarse space** an a priori estimate for the condition number is given by equation (2.27) in combination with either equation (2.29) or equation (2.30), respectively. The same can be said for the MsFEM and ACMS preconditioners. Despite this, there is no established method for estimating the full eigenspectrum. Without such an estimate, refining the CG iteration bound remains difficult. Overcoming this limitation is central to this work.

5

Preliminary Results

The results described in this chapter are adapted from the ideas discussed in [2, Section 4]. Therein Axelsson presents a sharpened CG iteration bound for two particular eigenspectra, which are described in section 5.1. The sharpened bound is then generalized to multiple clusters in section 5.2. The results are then compared with the classical CG iteration bound in section 5.3. Finally, the implications of the sharpened bound for the research questions are discussed in section 5.4.

5.1. Two cluster case

On the eigenspectrum of A , consider two intervals $[a, b]$ and $[c, d]$ with $0 < a < b < c < d$ such that all eigenvalues of A are contained in the union of these two intervals. Additionally, we have $\kappa(A) = \frac{d}{a}$. We treat the following two cases simultaneously

$$\sigma_1(A) = [a, b] \cup [c, d] \quad (5.1)$$

$$\sigma_2(A) = [c, d] \cup \bigcup_{\substack{i=1 \\ \lambda_i \in [a, b]}}^{N_{\text{tail}}} \lambda_i \quad (5.2)$$

where N_{tail} is the number of eigenvalues in the tail. The first case is a two-cluster eigenspectrum, while the second case has one cluster and a tail of eigenvalues.

In order to derive a CG iteration bound for these two cases we proceed as in the classical case laid out in 2.1.4. We know CG is optimal in the A -norm by equation (2.12), from which it follows that the error at the m^{th} iterate can be bounded as

$$\|e_m\|_A \leq \min_{r \in \mathcal{P}_m, r(0)=1} \max_{\lambda \in \sigma_i(A)} |r(\lambda)| \|e_0\|_A, \text{ for } i = 1, 2, \quad (5.3)$$

To get an upper bound for m equation (5.3) suggests we look for a polynomial $r_{\bar{m}}$ of degree \bar{m} that satisfies

$$\min_{r \in \mathcal{P}_{\bar{m}}, r(0)=1} \max_{\lambda \in \sigma_i(A)} |r(\lambda)| \leq \frac{\|e_m\|_A}{\|e_0\|_A} = \epsilon, \text{ for } i = 1, 2,$$

in which ϵ is the relative error.

Axelsson suggests we use not one monolithic residual polynomial function, but a multiplication of two residual polynomial functions $\hat{r}_p^{(i)}$ and $\hat{r}_{\bar{m}-p}$ for the two clusters. The superscript (i) corresponds to the two eigenspectra described above. The residual polynomial functions are defined as

$$\hat{r}_p^{(i)}(x) = \begin{cases} C_p \left(\frac{b+a-2x}{b-a} \right) / C_p \left(\frac{b+a}{b-a} \right), & \text{if } i = 1 \\ \prod_{i=1}^p (1 - x/\lambda_i), & \text{if } i = 2, p = N_{\text{tail}} \end{cases} \quad (5.4)$$

and

$$\hat{r}_{\bar{m}-p}(x) = C_{\bar{m}-p} \left(\frac{d+c-2x}{d-c} \right) / C_{\bar{m}-p} \left(\frac{d+c}{d-c} \right), \quad (5.5)$$

Indeed, the product $r_{\bar{m}} = \hat{r}_p \hat{r}_{\bar{m}-p} \in \mathcal{P}_{\bar{m}}$. Hence, we can use the residual polynomial functions to bound the error at the m^{th} iterate. Now, we obtain the following intermediate bounds

$$\max_{\lambda \in [a, b]} |r_{\bar{m}}(\lambda)| \leq \max_{\lambda \in [a, b]} |\hat{r}_p^{(i)}(\lambda)| \max_{\lambda \in [a, b]} |\hat{r}_{\bar{m}-p}(\lambda)| \leq \max_{\lambda \in [a, b]} |\hat{r}_p^{(i)}(\lambda)|, \text{ and} \quad (5.6a)$$

$$\max_{\lambda \in [c, d]} |r_{\bar{m}}(\lambda)| \leq \max_{\lambda \in [c, d]} |\hat{r}_p^{(i)}(\lambda)| \max_{\lambda \in [c, d]} |\hat{r}_{\bar{m}-p}(\lambda)| \leq \max_{\lambda \in [c, d]} |\hat{r}_p(\lambda)| / C_{\bar{m}-p} \left(\frac{d+c}{d-c} \right) \quad (5.6b)$$

where the first result follows from the fact that $|\hat{r}_{\bar{m}-p}(x)| < 1 \forall x \in [a, b]$ and the second result from

$$\left| C_{\bar{m}-p} \left(\frac{d+c-2x}{d-c} \right) \right| < 1 \forall x \in [c, d].$$

Furthermore, using the well-known inequality, we have

$$1/C_k \left(\frac{z_1 + z_2}{z_1 - z_2} \right) \leq 2 \left(\frac{\sqrt{z_2} - \sqrt{z_1}}{\sqrt{z_2} + \sqrt{z_1}} \right)^k, \text{ for } z_1 > z_2 > 0 \text{ and } k \in \mathbb{N}^+, \quad (5.7)$$

and

$$\max_{\lambda \in [a, b]} |\hat{r}_p^{(i)}(\lambda)| \leq \begin{cases} 2 \left(\frac{\sqrt{b} - \sqrt{a}}{\sqrt{b} + \sqrt{a}} \right)^p = \eta_1 & , \text{ if } i = 1, \\ \left(\frac{b}{a} - 1 \right)^p = \eta_2 & , \text{ if } i = 2, p = N_{\text{tail}}, \end{cases}$$

Note that if $i = 1$ we can determine p by requiring that the maximum of the residual polynomial function $\hat{r}_p^{(i)}$ in $[a, b]$ is equal to ϵ . This gives the following equation

$$p = \left\lceil \frac{1}{2} \sqrt{\frac{b}{a}} \ln \epsilon + 1 \right\rceil \quad (5.8)$$

Also note that for $i = 2$ $\hat{r}_p^{(2)}(\lambda) = 0$ for all eigenvalues $\lambda \in [a, b]$ and thereby, bounded by ϵ .

Next, $\hat{r}_p^{(i)}$ in $[c, d]$ is bounded by its maximum value within $[a, b]$ multiplied by the polynomial that is the fastest growing polynomial outside- and bounded below 1 within $[a, b]$. This polynomial is again the (transformed) Chebyshev polynomial $C_p \left(\frac{2x - b - a}{b - a} \right)$. Therefore,

$$\max_{\lambda \in [c, d]} |\hat{r}_p^{(i)}(\lambda)| \leq \eta_i C_p \left(\frac{2d - b - a}{b + a} \right)$$

At this point we have ensured equation (5.6a) is bounded by ϵ . So it remains to bound equation (5.6b). Using above results we can write

$$\max_{\lambda \in [c, d]} |r_{\bar{m}}(\lambda)| < \epsilon,$$

if we require that

$$\eta_i C_p \left(\frac{2d - b - a}{b - a} \right) / C_{\bar{m}-p} \left(\frac{d + c}{d - c} \right) < \epsilon. \quad (5.9)$$

Using that for $x_1, x_2, x_3 \in \mathbb{R}^+$ with $x_1 > x_3$ and $z = \frac{x_1 - x_2}{x_3}$

$$\begin{aligned} C_p(z) &\leq \left(z + \sqrt{z^2 - 1} \right)^p \\ &= \left(\frac{x_1 - x_2}{x_3} + \sqrt{\left[\frac{x_1 - x_2}{x_3} \right]^2 - 1} \right)^p \\ &\leq \left(\frac{x_1}{x_3} + \sqrt{\left[\frac{x_1}{x_3} \right]^2 - 1} \right)^p \\ &\leq \left(\frac{2x_1}{x_3} \right)^p, \end{aligned}$$

and substituting $x_1 = 2d$, $x_2 = b + a$ and $x_3 = b - a$ we obtain the following inequality

$$\eta_i \left(\frac{4d}{b - a} \right)^p / C_{\bar{m}-p} \left(\frac{d + c}{d - c} \right) < \epsilon.$$

Moreover,

$$\begin{aligned} \eta_i \left(\frac{4d}{b-a} \right)^p &= \begin{cases} 2 \left(\frac{\sqrt{b}-\sqrt{a}}{\sqrt{b}+\sqrt{a}} \frac{4d}{b-a} \right)^p, & \text{if } i = 1 \\ \left(\frac{b-a}{a} \frac{4d}{b-a} \right)^p, & \text{if } i = 2, \end{cases} \\ &= \begin{cases} 2 \left(\frac{4d}{b+2\sqrt{ab}+a} \right)^p, & \text{if } i = 1 \\ \left(\frac{4d}{a} \right)^p, & \text{if } i = 2, \end{cases} \\ &\leq 2 \begin{cases} \left(\frac{4d}{b} \right)^p, & \text{if } i = 1 \\ \left(\frac{4d}{a} \right)^p, & \text{if } i = 2, \end{cases} \end{aligned}$$

We can therefore require that the error bound above is satisfied if we have

$$1/C_{\bar{m}-p} \left(\frac{d+c}{d-c} \right) \leq \frac{\epsilon}{2 \left(\frac{4d}{e_i} \right)^p},$$

where

$$e_i = \begin{cases} b, & \text{if } i = 1 \\ a, & \text{if } i = 2. \end{cases}$$

Again using equation (5.7) and solving for the degree $\bar{m} - p$ we obtain

$$\bar{m} - p \geq \frac{1}{2} \sqrt{\frac{d}{c}} \left(\ln \epsilon + p \ln \frac{4d}{e_i} \right),$$

which leads to the following bound for the number of iterations [2, Equation 4.4]

$$\bar{m} = \left\lceil \frac{1}{2} \sqrt{\frac{d}{c}} \ln(2/\epsilon) + \left(1 + \frac{1}{2} \sqrt{\frac{d}{c}} \ln(4d/e_i) \right) p \right\rceil, \quad (5.10)$$

where

$$1 \leq p \leq \min \left\{ \left\lceil \frac{1}{2} \sqrt{\frac{b}{a}} \ln \epsilon + 1 \right\rceil, N_{\text{tail}} \right\}.$$

5.2. Generalization to multiple clusters

At this point we assume that we are dealing with an eigenspectrum of the form $\sigma_1(A)$, i.e. we are only treating case 1. In section 5.4, it is reasoned that this is indeed a very applicable case for a discretized Darcy problem.

In this case, the technique outlined in section 5.1 starts at the left most cluster $[a, b]$, finds the Chebyshev degree $p_1 = p$ satisfying inequality 5.8, moves to the neighboring cluster $[c, d]$ and finds the Chebyshev degree $p_2 = \bar{m} - p$ satisfying inequality 5.9. Rewriting inequality 5.9 gives the following equation for p_2 :

$$\frac{1}{C_{p_2} \left(\frac{d+c}{d-c} \right)} \leq \frac{\epsilon}{C_{p_1}^{(1)}(d)} = \epsilon_2, \quad (5.11)$$

where

$$C_{p_1}^{(1)}(x) = C_{p_1} \left(\frac{b+a-2x}{b-a} \right) / C_{p_1} \left(\frac{b+a}{b-a} \right),$$

is the Chebyshev polynomial corresponding to the first cluster.

Suppose there is a third cluster next to $[c, d]$, i.e. $[e, f]$. We can repeat the process and find the Chebyshev degree p_3 satisfying a similar inequality as 5.11 for the third cluster.

$$\frac{1}{C_{p_3}\left(\frac{f+e}{f-e}\right)} \leq \frac{\epsilon}{C_{p_1}^{(1)}(f)C_{p_2}^{(2)}(f)} = \epsilon_3,$$

This leads to the general equation for the Chebyshev degree p_i of the i^{th} cluster $[a_i, b_i]$

$$\frac{1}{C_{p_i}\left(\frac{b_i+a_i}{b_i-a_i}\right)} \leq \frac{\epsilon}{\prod_{j=1}^{i-1} C_{p_j}^{(j)}(b_i)} = \epsilon_i. \quad (5.12)$$

Due to the large range of the Chebyshev polynomials \tilde{C}_p a computer is likely to result in floating point number overflow during calculation of the denominator of equation (5.12). Instead, we first apply inequality 5.7 and introduce the cluster condition numbers $\kappa_i = \frac{b_i}{a_i}$, where i is the index of the cluster. We can then rewrite equation (5.12) as follows

$$p_i = \left\lceil \ln \frac{\epsilon_i}{2} / \ln \frac{\sqrt{\kappa_i} - 1}{\sqrt{\kappa_i} + 1} \right\rceil,$$

and

$$\ln \frac{\epsilon_i}{2} = \ln \frac{\epsilon}{2} - \sum_{j=1}^{i-1} \ln C_{p_j}^{(j)}(b_i).$$

Let $z_1^{(i,j)} = \frac{b_j + a_j - 2b_i}{b_j - a_j}$ and $z_2^{(j)} = \frac{b_j + a_j}{b_j - a_j}$ then

$$\ln C_{p_j}^{(j)}(b_i) = \ln C_{p_j}(z_1^{(i,j)}) - \ln C_{p_j}(z_2^{(j)}).$$

We have, using the definition of the Chebyshev polynomial

$$\ln C_{p_j}(z_1^{(i,j)}) \lesssim p_j \ln \left[z_1^{(i,j)} - \sqrt{\left(z_1^{(i,j)}\right)^2 - 1} \right] - \ln 2, \quad (5.13)$$

and

$$\ln C_{p_j}(z_2^{(j)}) \gtrsim p_j \ln \left[z_2^{(j)} + \sqrt{\left(z_2^{(j)}\right)^2 - 1} \right] - \ln 2, \quad (5.14)$$

both of which become more accurate equalities as $z, m \rightarrow \infty$. Introducing

$$\begin{aligned} \zeta_1^{(i,j)} &= z_1^{(i,j)} - \sqrt{\left(z_1^{(i,j)}\right)^2 - 1}, \\ \zeta_2^{(j)} &= z_2^{(j)} + \sqrt{\left(z_2^{(j)}\right)^2 - 1}, \text{ and} \\ f_i &= \frac{\sqrt{\kappa_i} - 1}{\sqrt{\kappa_i} + 1}, \end{aligned}$$

with κ_i the i^{th} cluster condition number, and substituting the inequalities 5.13 and 5.14 back into the bound for p_i gives

$$\begin{aligned} p_i &\leq \left\lceil \frac{\ln \frac{\epsilon}{2} - \sum_{j=1}^{i-1} p_j \left\{ \ln \zeta_1^{(i,j)} - \ln \zeta_2^{(j)} \right\}}{\ln f_i} \right\rceil \\ &= \left\lceil \log_{f_i} \frac{\epsilon}{2} - \sum_{j=1}^{i-1} p_j \left\{ \log_{f_i} \zeta_1^{(i,j)} - \log_{f_i} \zeta_2^{(j)} \right\} \right\rceil \\ &= \left\lceil \log_{f_i} \frac{\epsilon}{2} - \sum_{j=1}^{i-1} p_j \log_{f_i} \frac{\zeta_1^{(i,j)}}{\zeta_2^{(j)}} \right\rceil \end{aligned}$$

Note that in general $\zeta_1^{(i,j)} < \zeta_2^{(j)}$ and hence $\log_{f_i} \frac{\zeta_2^{(j)}}{\zeta_1^{(i,j)}} > 0$. This prompts us to write

$$p_i \leq \left\lceil \log_{f_i} \frac{\epsilon}{2} + \sum_{j=1}^{i-1} p_j \log_{f_i} \frac{\zeta_2^{(j)}}{\zeta_1^{(i,j)}} \right\rceil \quad (5.15)$$

Evidently, adding more clusters to the left of the interval $[a_i, b_i]$ increases the degree p_i of the Chebyshev polynomial. Next to this, equation (5.15) reduces to the classical CG iteration bound equation (2.11) for a single cluster when $i = N_{\text{clusters}} = 1$.

Equation 5.15 gives us a way to calculate the Chebyshev degree p_i of the i^{th} cluster $[a_i, b_i]$ in terms of the Chebyshev degrees of the previous clusters. To obtain a bound on the number of iterations for the CG method we sum the Chebyshev degrees of all the clusters

$$\bar{m} = \sum_{i=1}^{N_{\text{clusters}}} p_i \quad (5.16)$$

5.3. Numerical experiments

Equations 5.15 and 5.16 give a sequential algorithm for determining an upper bound on the number of iterations for the CG method. Figure 5.1 compares this bound with the classical CG iteration bound equation (2.11). As is the case for figure 2.2, $m_{\text{classical}} = 26$

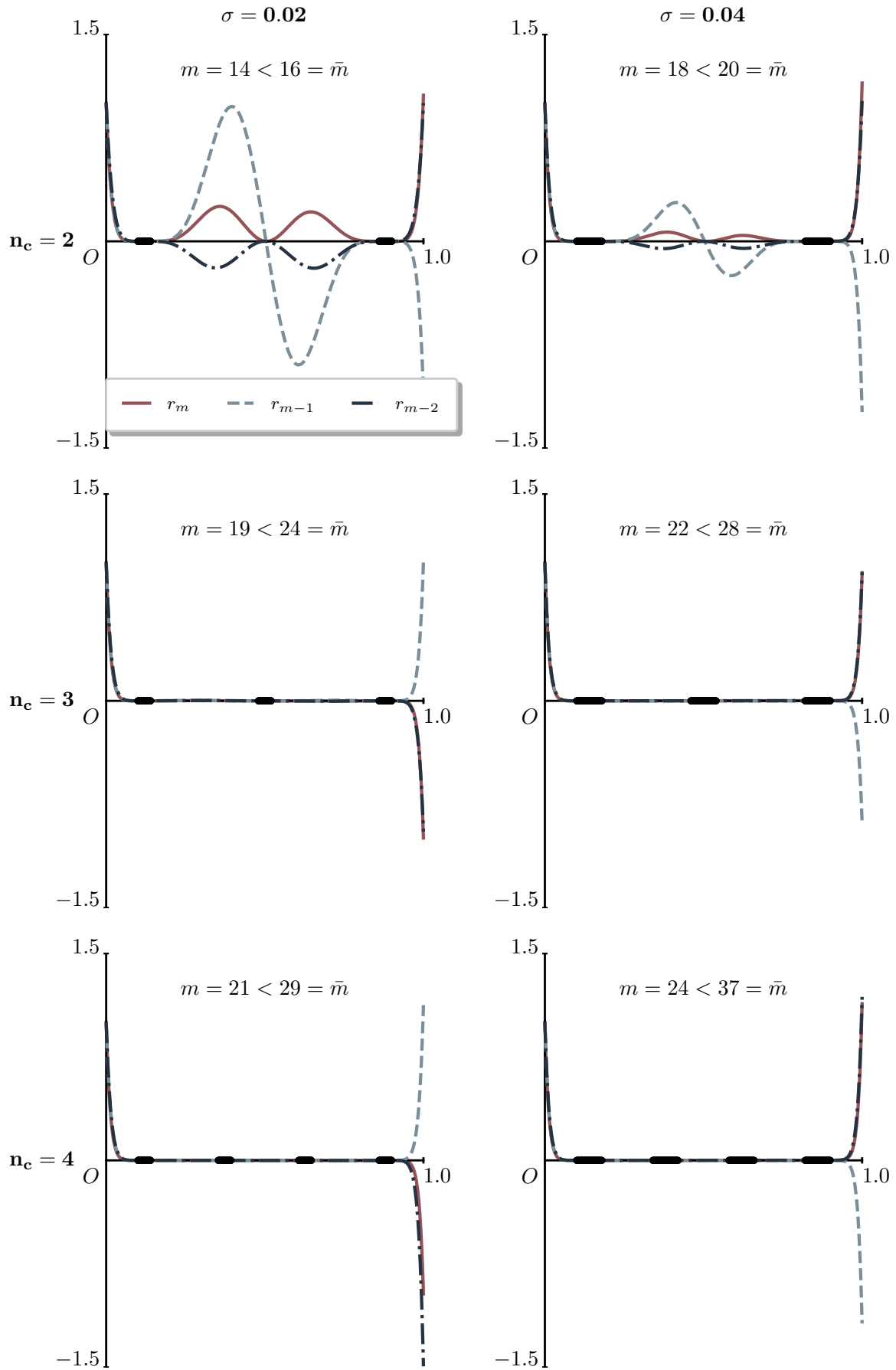


Figure 5.1: As in figure 2.2, plots of the last three CG residual polynomials for different eigenvalue distributions. n_c indicates the number of clusters and σ is the width of the cluster. The size of the system N and the condition number $\kappa(A)$ are kept constant. m indicates the number of iterations required for convergence. However, here \bar{m} is determined by equations (5.15) and (5.16).

Figure 5.1 shows that the sharpened CG iteration bound is significantly lower than the classical CG iteration bound for the two cluster case. The performance of the sharpened bound does decrease as the number of clusters increases, as is evident from equations (5.15) and (5.16). Performance also decreases as clusters become wider. So much so, that the sharpened bound is worse than the classical bound for the three cluster case with spread $\sigma = 0.04$ and for the four cluster case.

Worsening performance for the sharpened bound with increased cluster width is expected. Focussing on the two cluster case, we rediscover the ratios $\frac{d}{c}$ in equation (5.10) as well as $\frac{a}{b}$ in the corresponding equation for p . These ratios grow with increasing cluster width.

5.4. Implications for research

The preliminary results discussed in this chapter show that we can find both an a priori analytic two-cluster (equation (5.10)) and multiple-cluster (equation (5.16)) sharpened iteration bound for the CG method. The latter can also be implemented as a sequential, numerical algorithm that can be applied to artificially constructed spectra in figure 5.1. The sharpened bound appears to perform best in the two-cluster case, which has the most correspondence to the eigenspectrum of a typical (preconditioned) Darcy problem. Hence, **Q3** is answered positively.

With regard to **Q1**, the cluster condition number κ_i is introduced as a measure of the cluster width. This suggests that we can use the cluster condition number to distinguish between different preconditioners which is a promising result for **Q6**. Moreover, inspecting equation (5.10) more closely for the eigenspectrum in equation (5.1) (case $i = 1$) reveals the presence of a sort of spectral gap $\frac{d}{b}$. This serves as yet another candidate for a potential set of spectral characteristics to estimate the distribution of eigenvalues in the eigenspectrum.

A logical next step is to more rigorously investigate how the sharpened bound depends on κ_i as well as the spectral gap (**Q5**). Subsequently, we can simulate the eigenspectrum of a Darcy problem and compare the sharpened bound with the classical bound (**Q4**). This will lead to a clear understanding of the performance of the sharpened bound in the main problem context of this thesis: heterogeneous scalar elliptic problems with high-contrast coefficient.

Furthermore, we can construct, discretize, and precondition a model Darcy problem with the methods outlined in section 3.2. Then, we apply both the sharpened bound and the CG method to the resulting systems, and investigate how sharp the new bound is (**Q6**).

The main challenge described in section 4.4 still stands. More work is needed to be able to use the sharpened bound for spectra that are not known or artificially constructed beforehand. The results in this chapter suggest that the cluster condition number is a good candidate for a measure of the eigenspectrum. However, it is not yet clear how to estimate the cluster condition number for a general eigenspectrum. This is an important step towards answering **Q2**.

6

Conclusion

This thesis stresses that the classical condition number-based CG iteration bound does not fully capture the convergence behavior in high-contrast heterogeneous elliptic problems, particularly when Schwarz preconditioners are employed. By incorporating additional spectral characteristics, such as the distribution, clustering, and gaps of eigenvalues in the eigenspectrum, the refined bound offers a more accurate and discriminative measure of iterative performance. Preliminary results indicate that these spectral properties significantly influence the convergence rate and can be exploited to predict and compare the efficacy of different preconditioners.

Further research is required to test the refined bound on an eigenspectrum typically found in Darcy problems and to develop robust methods for estimating the full eigenspectrum in high-contrast problems found in practice. This research contributes to the theoretical understanding of iterative solvers and has practical importance for improving computational efficiency in solving complex elliptic PDEs.

Bibliography

- [1] Filipe A. C. S. Alves, Alexander Heinlein, and Hadi Hajibeygi. *A computational study of algebraic coarse spaces for two-level overlapping additive Schwarz preconditioners*. 2024. arXiv: 2408.08187 [math.NA]. URL (cit. on pp. 4, 23, 26).
- [2] O. Axelsson. “A class of iterative methods for finite element equations”. In: *Computer Methods in Applied Mechanics and Engineering* 9.2 (1976), pp. 123–137. issn: 0045-7825. doi: [https://doi.org/10.1016/0045-7825\(76\)90056-6](https://doi.org/10.1016/0045-7825(76)90056-6). URL (cit. on pp. 23, 28, 30).
- [3] B. Beckermann and A. B. J. Kuijlaars. “On The Sharpness of an Asymptotic Error Estimate for Conjugate Gradients”. In: *BIT Numerical Mathematics* 41.5 (2001), pp. 856–867 (cit. on p. 24).
- [4] Bernhard Beckermann and Arno B. J. Kuijlaars. “Superlinear CG Convergence for Special Right-Hand Sides”. In: *Electronic Transactions on Numerical Analysis* 14 (2002), pp. 1–19. issn: 1068-9613. URL (cit. on p. 24).
- [5] Bernhard Beckermann and Arno B. J. Kuijlaars. “Superlinear Convergence of Conjugate Gradients”. In: *SIAM Journal on Numerical Analysis* 39.1 (2001), pp. 300–329. doi: 10.1137/S0036142999363188. eprint: <https://doi.org/10.1137/S0036142999363188>. URL (cit. on p. 24).
- [6] Clark R. Dohrmann, Axel Klawonn, and Olof B. Widlund. “A family of energy minimizing coarse spaces for overlapping Schwarz preconditioners”. In: *Domain Decomposition Methods in Science and Engineering XVII*. Vol. 60. Lecture Notes in Computational Science and Engineering. St. Wolfgang / Strobl, Austria, 2008, pp. 247–254 (cit. on p. 23).
- [7] Clark R. Dohrmann and Olof B. Widlund. “On the Design of Small Coarse Spaces for Domain Decomposition Algorithms”. In: *SIAM Journal on Scientific Computing* 39.4 (2017), A1466–A1488. doi: 10.1137/17M1114272. eprint: <https://doi.org/10.1137/17M1114272>. URL (cit. on p. 23).
- [8] Victorita Dolean, Pierre Jolivet, and Frédéric Nataf. *An Introduction to Domain Decomposition Methods*. Philadelphia, PA: Society for Industrial and Applied Mathematics, 2015. doi: 10.1137/1.9781611974065. eprint: <https://epubs.siam.org/doi/pdf/10.1137/1.9781611974065>. URL (cit. on pp. 13–20).
- [9] Yalchin Efendiev, Juan Galvis, and Xiao-Hui Wu. “Multiscale finite element methods for high-contrast problems using local spectral basis functions”. In: *Journal of Computational Physics* 230.4 (2011), pp. 937–955. issn: 0021-9991. doi: <https://doi.org/10.1016/j.jcp.2010.09.026>. URL (cit. on p. 22).
- [10] I. G. Graham, P. O. Lechner, and R. Scheichl. “Domain decomposition for multiscale PDEs”. In: *Numerische Mathematik* 106 (2007), pp. 589–626. doi: 10.1007/s00211-007-0074-1. URL (cit. on p. 22).
- [11] Alexander Heinlein. “Multiscale coarse spaces for overlapping Schwarz methods based on the ACMS space in 2D”. en. In: (2018). Ed. by Lothar Reichel (Hg.) Ronny Ramlau, pp. 156–182. issn: 1068-9613. URL (cit. on pp. 4, 22).
- [12] Alexander Heinlein et al. “Adaptive GDSW Coarse Spaces of Reduced Dimension for Overlapping Schwarz Methods”. In: *SIAM Journal on Scientific Computing* 44.3 (2022), A1176–A1204. doi: 10.1137/20M1364540. eprint: <https://doi.org/10.1137/20M1364540>. URL (cit. on p. 23).
- [13] Thomas Y. Hou and Xiao-Hui Wu. “A Multiscale Finite Element Method for Elliptic Problems in Composite Materials and Porous Media”. In: *J. Comput. Phys.* 134.1 (June 1997), pp. 169–189. issn: 0021-9991. doi: 10.1006/jcph.1997.5682. URL (cit. on p. 22).
- [14] C. T. Kelley. *Iterative Methods for Linear and Nonlinear Equations*. Society for Industrial and Applied Mathematics, 1995. doi: 10.1137/1.9781611970944. eprint: <https://epubs.siam.org/doi/pdf/10.1137/1.9781611970944>. URL (cit. on p. 11).

- [15] Ivan Lunati and Seong H. Lee. “An Operator Formulation of the Multiscale Finite-Volume Method with Correction Function”. In: *Multiscale Modeling & Simulation* 8.1 (2009), pp. 96–109. doi: 10.1137/080742117. eprint: <https://doi.org/10.1137/080742117>. URL (cit. on p. 23).
- [16] Gérard Meurant and Zdeněk Strakoš. “The Lanczos and conjugate gradient algorithms in finite precision arithmetic”. In: *Acta Numerica* 15 (2006), pp. 471–542. doi: 10.1017/S096249290626001X (cit. on p. 8).
- [17] Yousef Saad. *Iterative Methods for Sparse Linear Systems*. Second. Society for Industrial and Applied Mathematics, 2003. doi: 10.1137/1.9780898718003. eprint: <https://epubs.siam.org/doi/pdf/10.1137/1.9780898718003>. URL (cit. on pp. 4–6, 13).
- [18] H.A. Schwarz. In: *Journal für die reine und angewandte Mathematik* 1869.70 (1869), pp. 105–120. doi: 10.1515/crll.1869.70.105. URL (cit. on p. 13).
- [19] Z. Strakoš. “On the real convergence rate of the conjugate gradient method”. In: *Linear Algebra and its Applications* 154-156 (1991), pp. 535–549. issn: 0024-3795. doi: [https://doi.org/10.1016/0024-3795\(91\)90393-B](https://doi.org/10.1016/0024-3795(91)90393-B). URL (cit. on p. 23).
- [20] Y. Wang, H. Hajibeygi, and H.A. Tchelepi. “Algebraic multiscale solver for flow in heterogeneous porous media”. English. In: *Journal of Computational Physics* 259. February (2014). Harvest, pp. 284–303. issn: 0021-9991. doi: 10.1016/j.jcp.2013.11.024 (cit. on p. 23).